

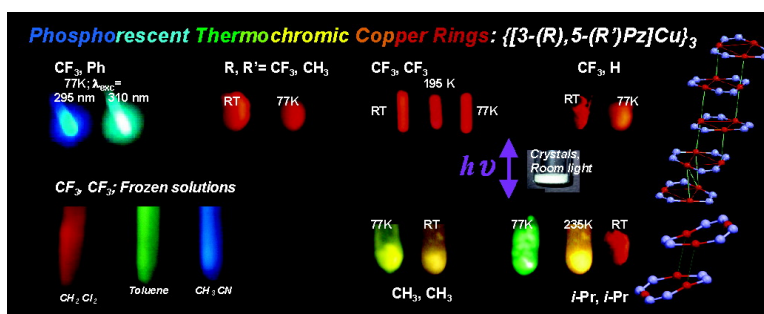
Article

## Brightly Phosphorescent Trinuclear Copper(I) Complexes of Pyrazolates: Substituent Effects on the Supramolecular Structure and Photophysics

H. V. Rasika Dias, Himashinie V. K. Diyabalanage, Maha G. Eldabaja, Oussama Elbjeirami, Manal A. Rawashdeh-Omary, and Mohammad A. Omary

*J. Am. Chem. Soc.*, **2005**, 127 (20), 7489-7501 • DOI: 10.1021/ja0427146 • Publication Date (Web): 29 April 2005

Downloaded from <http://pubs.acs.org> on March 25, 2009



### More About This Article

Additional resources and features associated with this article are available within the HTML version:

- Supporting Information
- Links to the 28 articles that cite this article, as of the time of this article download
- Access to high resolution figures
- Links to articles and content related to this article
- Copyright permission to reproduce figures and/or text from this article

[View the Full Text HTML](#)

## Brightly Phosphorescent Trinuclear Copper(I) Complexes of Pyrazolates: Substituent Effects on the Supramolecular Structure and Photophysics

H. V. Rasika Dias,<sup>\*,†</sup> Himashinie V. K. Diyabalanage,<sup>†</sup> Maha G. Eldabaja,<sup>‡</sup> Oussama Elbjairami,<sup>‡</sup> Manal A. Rawashdeh-Omary,<sup>‡</sup> and Mohammad A. Omary<sup>\*,‡</sup>

Contribution from the Department of Chemistry and Biochemistry, The University of Texas at Arlington, Arlington, Texas 76019, and Department of Chemistry, University of North Texas, Denton, Texas 76203

Received December 3, 2004; E-mail: dias@uta.edu; omary@unt.edu

**Abstract:** Synthetic details, solid-state structures, and photophysical properties of a group of trimeric copper(I) complexes containing pyrazolate ligands are described. The reaction of copper(I) oxide and the fluorinated pyrazoles [3-(CF<sub>3</sub>)Pz]H, [3-(CF<sub>3</sub>),5-(Me)Pz]H, and [3-(CF<sub>3</sub>),5-(Ph)Pz]H leads to the corresponding trinuclear copper(I) pyrazolates, {[3-(CF<sub>3</sub>)Pz]Cu}<sub>3</sub>, {[3-(CF<sub>3</sub>),5-(Me)Pz]Cu}<sub>3</sub>, and {[3-(CF<sub>3</sub>),5-(Ph)Pz]Cu}<sub>3</sub>, respectively, in high yield. The {[3,5-(*i*-Pr)<sub>2</sub>Pz]Cu}<sub>3</sub> compound was obtained by a reaction between [Cu(CH<sub>3</sub>CN)<sub>4</sub>][BF<sub>4</sub>], [3,5-(*i*-Pr)<sub>2</sub>Pz]H, and NEt<sub>3</sub>. These compounds as well as {[3,5-(Me)<sub>2</sub>Pz]Cu}<sub>3</sub> and {[3,5-(CF<sub>3</sub>)<sub>2</sub>Pz]Cu}<sub>3</sub> adopt trimeric structures with nine-membered Cu<sub>3</sub>N<sub>6</sub> metallacycles. There are varying degrees and types of intertrimer Cu...Cu interactions. These contacts give rise to zigzag chains in the fluorinated complexes, {[3-(CF<sub>3</sub>)Pz]Cu}<sub>3</sub>, {[3-(CF<sub>3</sub>),5-(Me)Pz]Cu}<sub>3</sub>, {[3-(CF<sub>3</sub>),5-(Ph)Pz]Cu}<sub>3</sub>, and {[3,5-(CF<sub>3</sub>)<sub>2</sub>Pz]Cu}<sub>3</sub>, whereas the nonfluorinated complexes, {[3,5-(Me)<sub>2</sub>Pz]Cu}<sub>3</sub> and {[3,5-(*i*-Pr)<sub>2</sub>Pz]Cu}<sub>3</sub> form dimers of trimers. Out of all the compounds examined in this study, {[3-(CF<sub>3</sub>),5-(Ph)Pz]Cu}<sub>3</sub> has the longest (3.848 Å) and {[3,5-(Me)<sub>2</sub>Pz]Cu}<sub>3</sub> has the shortest (2.946 Å) next-neighbor intertrimer Cu...Cu distance. The Cu...Cu separations within the trimer units do not vary significantly (typically 3.20–3.26 Å). All of these trinuclear copper(I) pyrazolates show bright luminescence upon exposure to UV radiation. The luminescence bands are hugely red-shifted from the corresponding lowest-energy excitations, rather broad, and unstructured even at low temperatures, suggesting metal-centered emissions owing to intertrimer Cu...Cu interactions that are strengthened in the phosphorescent state. The {[3-(CF<sub>3</sub>),5-(Ph)Pz]Cu}<sub>3</sub> compound exhibits an additional highly structured phosphorescence with a vibronic structure corresponding to the pyrazolyl (Pz) ring. The luminescence properties of solids and solutions of the trimeric compounds in this study show fascinating trends with dramatic sensitivities to temperature, solvent, concentration, and excitation wavelengths.

### Introduction

The structure and properties of copper pyrazolates are of significant interest.<sup>1</sup> These compounds have been found to exhibit a variety of structures ranging from polymers to trimers with exo-bidentate coordination of the pyrazolate ligand to the copper centers.<sup>1–15</sup> For instance, [Cu(Pz)]<sub>n</sub> (**1**) (Pz = pyrazolate)

is polymeric and exists in two distinct crystalline phases, α-[Cu(Pz)]<sub>n</sub> and β-[Cu(Pz)]<sub>n</sub>, which differ in the interchain Cu...Cu contacts.<sup>11</sup> Structurally characterized trinuclear copper(I) pyrazolates containing nine-membered Cu<sub>3</sub>N<sub>6</sub> metallacycles include {[3,5-(Me)<sub>2</sub>Pz]Cu}<sub>3</sub>,<sup>3</sup> {[3,4,5-(Me)<sub>3</sub>Pz]Cu}<sub>3</sub>,<sup>10</sup> {[3,5-(Me)<sub>2</sub>,4-(NO<sub>2</sub>)Pz]Cu}<sub>3</sub> (**2**),<sup>8</sup> {[3,5-(*i*-Pr)<sub>2</sub>Pz]Cu}<sub>3</sub>,<sup>12</sup> and {[3,5-(CF<sub>3</sub>)<sub>2</sub>Pz]Cu}<sub>3</sub>.<sup>5</sup> The trimeric compound, {[2-(3-Pz)Py]Cu}<sub>3</sub>, has a pyridyl sidearm.<sup>16,17</sup> Larger substituents in the 3-, 4-, and 5-positions at the pyrazole ring lead to tetrameric structures such as in {[3,5-(*t*-Bu)<sub>2</sub>Pz]Cu}<sub>4</sub> (**3**),<sup>12,14</sup> {[3-(*i*-Pr),5-(*t*-Bu)Pz]Cu}<sub>4</sub>,<sup>12</sup> {[3,5-(carbo-*sec*-butoxy)<sub>2</sub>Pz]Cu}<sub>4</sub>,<sup>14</sup> and {[3,5-(*i*-Pr)<sub>2</sub>,4-(Br)Pz]Cu}<sub>4</sub>.<sup>18</sup> A tetramer and a trimer derived from the same

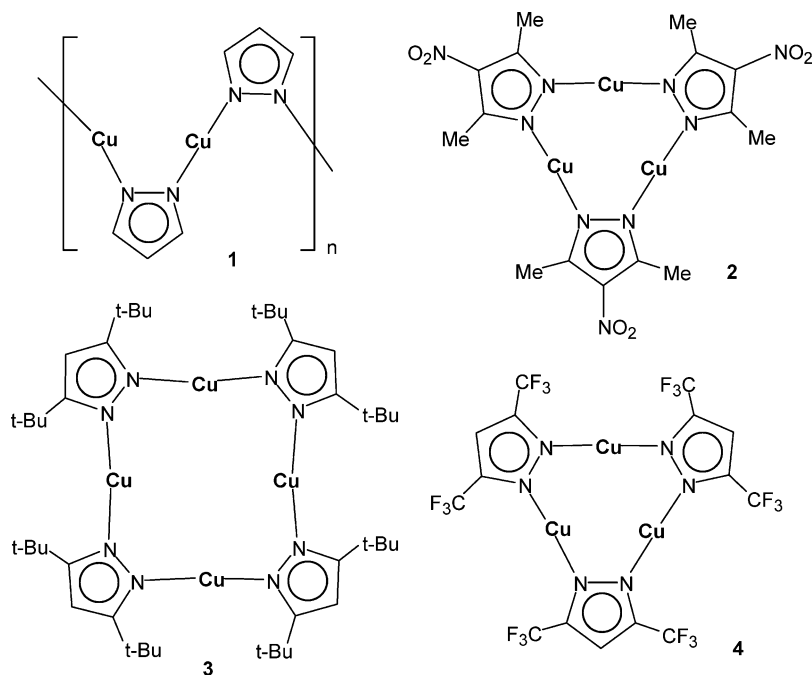
<sup>†</sup> The University of Texas at Arlington.

<sup>‡</sup> University of North Texas.

- (1) La Monica, G.; Ardizzoia, G. A. *Prog. Inorg. Chem.* **1997**, *46*, 151–238.
- (2) Ardizzoia, G. A.; Monica, G. L. *Inorg. Synth.* **1997**, *31*, 299–302.
- (3) Ehlert, M. K.; Rettig, S. J.; Storr, A.; Thompson, R. C.; Trotter, J. *Can. J. Chem.* **1990**, *68*, 1444–1449.
- (4) Ehlert, M. K.; Storr, A.; Thompson, R. C. *Can. J. Chem.* **1992**, *70*, 1121–1128.
- (5) Dias, H. V. R.; Polach, S. A.; Wang, Z. *J. Fluor. Chem.* **2000**, *103*, 163–169.
- (6) Ardizzoia, G. A.; Cenini, S.; La Monica, G.; Masciocchi, N.; Moret, M. *Inorg. Chem.* **1994**, *33*, 1458–1463.
- (7) Raptis, R. G.; Fackler, J. P., Jr. *Inorg. Chem.* **1988**, *27*, 4179–4182.
- (8) Ardizzoia, G. A.; Cenini, S.; La Monica, G.; Masciocchi, N.; Maspero, A.; Moret, M. *Inorg. Chem.* **1998**, *37*, 4284–4292.
- (9) Meyer, F.; Jacobi, A.; Zsolnai, L. *Chem. Ber.* **1997**, *130*, 1441–1447.
- (10) Ehlert, M. K.; Rettig, S. J.; Storr, A.; Thompson, R. C.; Trotter, J. *Can. J. Chem.* **1992**, *70*, 2161–2173.
- (11) Masciocchi, N.; Moret, M.; Cairati, P.; Sironi, A.; Ardizzoia, G. A.; La Monica, G. *J. Am. Chem. Soc.* **1994**, *116*, 7668–7676.

- (12) Fujisawa, K.; Ishikawa, Y.; Miyashita, Y.; Okamoto, K.-i. *Chem. Lett.* **2004**, *33*, 66–67.
- (13) Ardizzoia, G. A.; Beccalli, E. M.; La Monica, G.; Masciocchi, N.; Moret, M. *Inorg. Chem.* **1992**, *31*, 2706–2711.
- (14) Maspero, A.; Brenna, S.; Galli, S.; Penoni, A. *J. Organomet. Chem.* **2003**, *672*, 123–129.
- (15) Enomoto, M.; Kishimura, A.; Aida, T. *J. Am. Chem. Soc.* **2001**, *123*, 5608–5609.
- (16) Singh, K.; Long, J. R.; Stavropoulos, P. *J. Am. Chem. Soc.* **1997**, *119*, 2942–2943.
- (17) Singh, K.; Long, J. R.; Stavropoulos, P. *Inorg. Chem.* **1998**, *37*, 1073–1079.

Chart 1



pyrazolate ligand are also known (e.g., {[3,5-(Ph)<sub>2</sub>Pz]Cu}<sub>4</sub> and {[3,5-(Ph)<sub>2</sub>Pz]Cu}<sub>3</sub>).<sup>6,7</sup> Apart from the interests related to structural diversity, some of these copper pyrazolates have been utilized for examining interactions between closed-shell d<sup>10</sup> copper systems,<sup>16,17</sup> catalytic applications,<sup>6,14</sup> and as luminescent materials.<sup>15,19</sup> Copper(I) pyrazolates also serve as excellent precursors to obtain various mixed ligand complexes of copper, for example, {[3,5-(CF<sub>3</sub>)<sub>2</sub>Pz]Cu(2,4,6-collidine)}<sub>2</sub> and {[3,5-(Me)<sub>2</sub>,4-(NO<sub>2</sub>)Pz]Cu(CNCy)<sub>2</sub>}<sub>2</sub>.<sup>8,20</sup>

An area of research focus in our laboratories concerns structural and spectroscopic studies of copper complexes featuring fluorinated pyrazolates.<sup>19,20</sup> In contrast to the nonfluorinated analogues, copper complexes of fluorinated pyrazolates are rare.<sup>1,2</sup> Dias et al. have described the synthesis of a copper(I) complex containing a heavily fluorinated pyrazolate, {[3,5-(CF<sub>3</sub>)<sub>2</sub>Pz]Cu}<sub>3</sub> (**4**).<sup>5</sup> We have recently communicated that solids and glassy solutions of this molecule exhibit bright luminescence that can be fine- and coarse-tuned to multiple bright visible colors by varying the solvent, concentration, temperature, and excitation wavelength.<sup>19</sup> These types of neutral metal complexes containing fluorinated ligands are of particular interest as emitting materials for molecular light-emitting devices (MOLEDs) because fluorination facilitates thin-film fabrication and because the presence of a closed-shell transition metal should enhance the phosphorescence.<sup>21–25</sup> Fluorinated ligands also endow other beneficial properties to metal adducts, such as improved thermal and oxidative stability and reduced concentration quenching.<sup>23–27</sup>

An interesting study of the luminescence properties of copper(I) pyrazolates was reported recently by Aida et al.<sup>15</sup> Although these molecules do not contain fluorinated ligands, they demonstrated that poly(benzyl ether)-substituted pyrazolate adducts of copper(I) can be employed to form brightly luminescent superhelical fibers. It is also noteworthy that in contrast to the Au<sup>I</sup> adducts, photophysical studies of such trimetallic species involving the lighter coinage metal family members, Cu<sup>I</sup> and Ag<sup>I</sup>, have not received much attention.<sup>28–30</sup> In this paper, we describe the synthesis of several trimeric copper(I) adducts of fluorinated pyrazolates, their solid-state structures, and photophysical properties. To investigate the possible effects of the electron-withdrawing and -donating substituents on the luminescence and structure of these materials, we also include in this study the nonfluorinated compounds, {[3,5-(Me)<sub>2</sub>Pz]Cu}<sub>3</sub> and {[3,5-(*i*-Pr)<sub>2</sub>Pz]Cu}<sub>3</sub>.<sup>3,12</sup>

## Experimental Section

**General Procedures.** All manipulations were carried out under an atmosphere of purified nitrogen using standard Schlenk techniques. Solvents were purchased from commercial sources, distilled from conventional drying agents, and degassed by the freeze–pump–thaw method twice prior to use. The glassware was oven-dried at 150 °C overnight. NMR spectra were recorded at 25 °C on a JEOL Eclipse 500 spectrometer (<sup>1</sup>H, 500.16 MHz; <sup>13</sup>C, 125.78 MHz; <sup>19</sup>F, 470.62 MHz). Proton and carbon chemical shifts are reported in parts per million versus Me<sub>4</sub>Si. <sup>19</sup>F NMR chemical shifts were referenced relative to external CFCl<sub>3</sub>. Infrared spectra were recorded on a JASCO FT-IR 410 spectrometer. Melting points were obtained on a Mel-Temp II

- (18) Dias, H. V. R.; Diyabalanage, H. V. K. Unpublished results.  
 (19) Dias, H. V. R.; Diyabalanage, H. V. K.; Rawashdeh-Omary, M. A.; Franzman, M. A.; Omary, M. A. *J. Am. Chem. Soc.* **2003**, *125*, 12072–12073.  
 (20) Omary, M. A.; Rawashdeh-Omary, M. A.; Diyabalanage, H. V. K.; Dias, H. V. R. *Inorg. Chem.* **2003**, *42*, 8612–8614.  
 (21) Haneline, M. R.; Tsunoda, M.; Gabbaie, F. P. *J. Am. Chem. Soc.* **2002**, *124*, 3737–3742.  
 (22) Omary, M. A.; Kassab, R. M.; Haneline, M. R.; Elbjairami, O.; Gabbaie, F. P. *Inorg. Chem.* **2003**, *42*, 2176–2178.  
 (23) Adachi, C.; Baldo, M. A.; Forrest, S. R. *J. Appl. Phys.* **2000**, *87*, 8049–8055.  
 (24) Grushin, V. V.; Herron, N.; LeCloux, D. D.; Marshall, W. J.; Petrov, V. A.; Wang, Y. *Chem. Commun.* **2001**, 1494–1495.

- (25) Zhang, J.; Kan, S.; Ma, Y.; Shen, J.; Chan, W.; Che, C. *Synth. Metals* **2001**, *121*, 1723–1724 and references therein.  
 (26) Dias, H. V. R.; Lu, H.-L.; Kim, H.-J.; Polach, S. A.; Goh, T. K. H. H.; Browning, R. G.; Lovely, C. J. *Organometallics* **2002**, *21*, 1466–1473 and references therein.  
 (27) Dias, H. V. R.; Kim, H.-J.; Lu, H.-L.; Rajeshwar, K.; de Tacconi, N. R.; Derecskei-Kovacs, A.; Marynick, D. S. *Organometallics* **1996**, *15*, 2994–3003 and references therein.  
 (28) Yam, V. W.-W.; Lo, K. K. W. *Mol. Supramol. Photochem.* **1999**, *4*, 31–112.  
 (29) Yam, V. W.-W.; Lo, K. K.-W. *Chem. Soc. Rev.* **1999**, *28*, 323–334.  
 (30) Ford, P. C.; Cariati, E.; Bourassa, J. *Chem. Rev.* **1999**, *99*, 3625–3648.

apparatus and were not corrected. Elemental analyses were performed using a Perkin-Elmer Model 2400 CHN analyzer. Cu<sub>2</sub>O was purchased from commercial sources. [3-(CF<sub>3</sub>)Pz]H,<sup>31</sup> [3-(CF<sub>3</sub>),5-(Me)Pz]H,<sup>32</sup> and [3-(CF<sub>3</sub>),5-(Ph)Pz]H<sup>33</sup> were prepared by published methods. {[3,5-(CF<sub>3</sub>)<sub>2</sub>Pz]Cu}<sub>3</sub><sup>5</sup> and {[3,5-(Me)<sub>2</sub>Pz]Cu}<sub>3</sub><sup>3</sup> were isolated using slightly modified literature procedures as described below. Tetrakis(acetonitrile)-copper(I) tetrafluoroborate was prepared by following a procedure analogous to that reported for [Cu(CH<sub>3</sub>CN)<sub>4</sub>](PF<sub>6</sub>) but employing aqueous HBF<sub>4</sub> instead of HPF<sub>6</sub>.<sup>34</sup>

**{[3-(CF<sub>3</sub>)Pz]Cu}<sub>3</sub>**: Cu<sub>2</sub>O (0.29 g, 1.90 mmol), 3-trifluoromethylpyrazole (0.50 g, 3.68 mmol), and acetonitrile (0.25 mL) were mixed in about 40.0 mL of degassed benzene. The resulting mixture was heated at 50–60 °C overnight under nitrogen. After cooling, the solution was filtered through a bed of Celite to remove some insoluble material. The filtrate was collected, and the solvent was removed under reduced pressure to obtain crude {[3-(CF<sub>3</sub>)Pz]Cu}<sub>3</sub> as a colorless solid. X-ray quality crystals were grown from hexane at 5 °C. Yield: 85%. Mp: 156–157 °C. <sup>1</sup>H NMR (CDCl<sub>3</sub>): δ 6.65 (br s, 3H, H<sub>4</sub>), 7.67 (br s, 3H, H<sub>5</sub>). <sup>13</sup>C{<sup>1</sup>H} NMR (CDCl<sub>3</sub>): δ 104.3 (Pz-C<sub>4</sub>), 122.0 (CF<sub>3</sub>, q, <sup>1</sup>J<sub>CF</sub> = 268 Hz), 140.2 (Pz-C<sub>5</sub>), 141.1, (CCF<sub>3</sub>, q, <sup>2</sup>J<sub>CF</sub> = 36.0 Hz). <sup>19</sup>F NMR (CDCl<sub>3</sub>): δ -61.4. IR (KBr, cm<sup>-1</sup>): 3853, 3745, 3159, 2962, 1735, 1653, 1521, 1457, 1380, 1350, 1308, 1240, 1171, 1154, 1121, 1083, 1003, 957, 879, 782, 743, 719, 656, 550. Anal. Calcd for C<sub>12</sub>H<sub>6</sub>F<sub>9</sub>N<sub>6</sub>Cu<sub>3</sub>: C, 24.19; H, 1.01; N, 14.10. Found: C, 24.32; H, 1.31; N, 14.20.

**{[3-(CF<sub>3</sub>),5-(Me)Pz]Cu}<sub>3</sub>**: Cu<sub>2</sub>O (0.15 g, 1.11 mmol) and 3-trifluoromethyl-5-methylpyrazole (0.50 g, 3.33 mmol) were mixed in benzene (40.0 mL). Acetonitrile (1.00 mL) was added, and the resulting mixture was refluxed for 12 h. After cooling, the solution was filtered through a bed of Celite to remove some insoluble material. The filtrate was collected, and the solvent was removed under reduced pressure to obtain crude {[3-(CF<sub>3</sub>),5-(Me)Pz]Cu}<sub>3</sub> as a colorless solid. X-ray quality crystals were obtained from dichloromethane at 5 °C. Yield: 92%. Mp: 214–215 °C. <sup>1</sup>H NMR (CDCl<sub>3</sub>): δ 2.28 (s, 6H, CH<sub>3</sub>), 2.32 (s, 3H, CH<sub>3</sub>), 6.37 (s, 3H, H<sub>4</sub>). <sup>13</sup>C{<sup>1</sup>H} NMR (CDCl<sub>3</sub>): δ 13.0 (s, CH<sub>3</sub>), 103.5 (Pz-C<sub>4</sub>), 121.1 (CF<sub>3</sub>, q, <sup>1</sup>J<sub>CF</sub> = 276 Hz), 143.2 (CCF<sub>3</sub>, q, <sup>2</sup>J<sub>CF</sub> = 39 Hz), 150.6 (s, CCH<sub>3</sub>). <sup>19</sup>F NMR (CDCl<sub>3</sub>): δ -59.8 (br s, CF<sub>3</sub>, 6F), -60.4 (br s, CF<sub>3</sub>, 3F). IR (KBr, cm<sup>-1</sup>): 3608, 3132, 2925, 1597, 1539, 1350, 1244, 1169, 1128, 1083, 1010, 798, 761, 719, 685, 664. Anal. Calcd for C<sub>15</sub>H<sub>12</sub>F<sub>9</sub>N<sub>6</sub>Cu<sub>3</sub>: C, 28.24; H, 1.90; N, 13.17. Found: C, 28.20; H, 1.74; N, 13.33.

**{[3-(CF<sub>3</sub>),5-(Ph)Pz]Cu}<sub>3</sub>**: Cu<sub>2</sub>O (0.14 g, 4.72 mmol) and 3-trifluoromethyl-5-phenylpyrazole (1.00 g, 4.72 mmol) were mixed in about 40.0 mL of benzene. Acetonitrile (0.25 mL) was added, and the resulting mixture was refluxed for 12 h. After cooling, the solution was filtered through a bed of Celite to remove some insoluble material. The filtrate was collected, and the solvent was removed under reduced pressure to obtain crude {[3-(CF<sub>3</sub>),5-(Ph)Pz]Cu}<sub>3</sub> as a colorless solid. X-ray quality crystals were obtained from hexane at 5 °C. Yield: 90%. Mp: 123–125 °C. <sup>1</sup>H NMR (CDCl<sub>3</sub>): δ 6.69 (s, 3H, H<sub>4</sub>), 7.42 (m, 9H, Ph), 7.54 (m, 6H, Ph). <sup>13</sup>C{<sup>1</sup>H} NMR (CDCl<sub>3</sub>): δ 102.1 (Pz-C<sub>4</sub>), 121.0 (CF<sub>3</sub>, q, <sup>1</sup>J<sub>CF</sub> = 250 Hz), 126.2, 129.3, 129.6, 144.5 (CCF<sub>3</sub>, q, <sup>2</sup>J<sub>CF</sub> = 37 Hz), 145.6, 149.2. <sup>19</sup>F NMR (CDCl<sub>3</sub>): δ -61.2. IR (KBr, cm<sup>-1</sup>): 3120, 2956, 1734, 1438, 1346, 1279, 1254, 1154, 1065, 1020, 985, 913, 841, 809, 760, 719, 690, 507. Anal. Calcd for C<sub>30</sub>H<sub>18</sub>F<sub>9</sub>N<sub>6</sub>Cu<sub>3</sub>: C, 43.72; H, 2.20; N, 10.20. Found: C, 44.10; H, 2.05; N, 9.98.

**{[3,5-(CF<sub>3</sub>)<sub>2</sub>Pz]Cu}<sub>3</sub>**: This compound could be obtained from a reaction between [3,5-(CF<sub>3</sub>)<sub>2</sub>Pz]H and copper(I) oxide in benzene, as reported earlier.<sup>5</sup> However, for some reason, certain runs gave fairly low yields of the expected trimer. We found that this problem could be solved by using benzene containing a few drops of CH<sub>3</sub>CN as the

reaction medium (see the procedure for {[3-(CF<sub>3</sub>)Pz]Cu}<sub>3</sub>). {[3,5-(CF<sub>3</sub>)<sub>2</sub>Pz]Cu}<sub>3</sub> can be purified either by recrystallizing using hexane or by vacuum sublimation at 80 °C/3.0 mmHg. Mp: 188–190 °C.

**{[3,5-(Me)<sub>2</sub>Pz]Cu}<sub>3</sub>**: This was prepared using the published procedure.<sup>3</sup> It produces a mixture of colorless trimers, {[3,5-(Me)<sub>2</sub>Pz]Cu}<sub>3</sub>, and a brown–red, polymeric solid with a composition {[3,5-(Me)<sub>2</sub>Pz]<sub>2</sub>Cu}<sub>n</sub>. Due to the high insolubility, it is difficult to separate the desired product from the crude mixture. Usually, the trimer separation has been achieved by manually separating the crystals. However, we found that the trimers could be obtained very conveniently in pure form by the vacuum sublimation of the crude mixture at 245 °C/3 mmHg. Mp: 325–327 °C.

**{[3,5-(i-Pr)<sub>2</sub>Pz]Cu}<sub>3</sub>**: A 100 mL, two-necked, round-bottomed flask equipped with a magnetic stirrer was connected to a nitrogen line. The flask was purged thoroughly with nitrogen and charged with 3,5-diisopropylpyrazole (0.50 g, 3.30 mmol) and acetone (20.0 mL). [Cu(CH<sub>3</sub>CN)<sub>4</sub>][BF<sub>4</sub>] (0.52 g, 1.65 mmol) was added while stirring. After the solution became clear, degassed triethylamine (1.0 mL) was added to the mixture over a period of 1 min. The product precipitated as a white solid. The resulting suspension was stirred for 30 min and then filtered. The product was washed with acetone (15.0 mL) and hexane (5.0 mL) and dried under reduced pressure. X-ray quality crystals were obtained from hexane at 5 °C. Yield: 88%. Mp: 158–160 °C. <sup>1</sup>H NMR (CDCl<sub>3</sub>): δ 1.34 (d, 36H, J = 6.5 Hz, CH<sub>3</sub>), 3.08 (septet, 6H, CH), 5.91 (s, 3H, H<sub>4</sub>). <sup>13</sup>C{<sup>1</sup>H} NMR (CDCl<sub>3</sub>): δ 23.6 (CH<sub>3</sub>), 28.7 (CH), 96.3 (s, Pz-C<sub>4</sub>), 160.7 (C-iPr). IR (KBr, cm<sup>-1</sup>): 3608, 3583, 2925, 2855, 2723, 1996, 1734, 1717, 1699, 1685, 1653, 1558, 1540, 1522, 1459, 1377, 1300, 1174, 1104, 1051, 796, 779. Anal. Calcd for C<sub>27</sub>H<sub>45</sub>N<sub>6</sub>Cu<sub>3</sub>: C, 50.33; H, 7.04; N, 13.04. Found: C, 50.43; H, 7.30; N, 13.12.

**X-ray Structure Determination.** A suitable crystal covered with a layer of hydrocarbon oil was selected and mounted with paratone-N oil on a cryo-loop and immediately placed in the low-temperature nitrogen stream. The X-ray intensity data were measured at 100(2) K on a Bruker SMART APEX CCD area detector system equipped with an Oxford Cryosystems 700 series Cryostream cooler, a graphite monochromator, and a Mo Kα fine-focus sealed tube (λ = 0.710 73 Å). The detector was placed at a distance of 5.995 cm from the crystal. The data frames were integrated with the Bruker SAINT-Plus software package. The data were corrected for absorption effects using the multiscan technique (SADABS).

Compounds {[3-(CF<sub>3</sub>),5-(Me)Pz]Cu}<sub>3</sub>, {[3-(CF<sub>3</sub>),5-(Ph)Pz]Cu}<sub>3</sub>, {[3,5-(CF<sub>3</sub>)<sub>2</sub>Pz]Cu}<sub>3</sub>, and {[3,5-(i-Pr)<sub>2</sub>Pz]Cu}<sub>3</sub> form good quality crystals for crystallography. Data collection for these compounds and the structure solution and refinement proceeded smoothly. {[3-(CF<sub>3</sub>)Pz]Cu}<sub>3</sub> forms small, very thin needles. Nevertheless, we were able to collect sufficient data for {[3-(CF<sub>3</sub>)Pz]Cu}<sub>3</sub> and solve the structure, as well. It crystallizes with two {[3-(CF<sub>3</sub>)Pz]Cu}<sub>3</sub> moieties in the asymmetric unit. The structures of compounds described in this manuscript were solved and refined using the Bruker SHELXTL (version 6.14) software package. All the non-hydrogen atoms were refined anisotropically. The hydrogen atoms were included at calculated positions during the refinement. Further details of the data collection and refinements are given in Table 1.

**Photophysical Measurements.** Steady-state luminescence spectra were acquired with a PTI QuantaMaster Model QM-4 scanning spectrofluorometer. The excitation and emission spectra were corrected for the wavelength-dependent lamp intensity and detector response, respectively. Lifetime data were acquired using fluorescence and phosphorescence subsystem add-ons to the PTI instrument. The pulsed excitation source was generated using the 337.1 nm line of the N<sub>2</sub> laser pumping a freshly prepared 1 × 10<sup>-2</sup> M solution of the continuum laser dye, Coumarin-540A, in ethanol, the output of which was appropriately tuned and frequency doubled to attain the excitation wavelengths needed based on the luminescence excitation spectra for each compound. Cooling in temperature-dependent measurements for the crystals was achieved using an Oxford optical cryostat, model Optistat CF ST, interfaced with a liquid nitrogen or liquid helium tank. Absorption spectra were acquired with a Perkin-Elmer Lambda 900

(31) Gerus, I. I.; Gorbunova, M. G.; Vdovenko, S. I.; Yagupol'skii, Y. L.; Kukhar, V. P. *Zh. Org. Khim.* **1990**, *26*, 1877–1883.

(32) Atwood, L. J.; Dixon, K. R.; Eadie, D. T.; Stobart, S. R.; Zaworotko, M. J. *Inorg. Chem.* **1983**, *22*, 774–779. (Mp: 80–82 °C. <sup>1</sup>H NMR (CDCl<sub>3</sub>): δ 2.33 (s, 3H, CH<sub>3</sub>), 6.30 (s, 1H, H<sub>4</sub>), 12.4 (br s, NH). <sup>19</sup>F NMR (CDCl<sub>3</sub>): δ -61.7.)

(33) Dias, H. V. R.; Goh, T. K. H. *Polyhedron* **2004**, *23*, 273–282, and references therein.

(34) Kubas, G. J. *Inorg. Synth.* **1979**, *19*, 90–92.



**Table 1.** X-ray Crystallographic Data for {[3-(CF<sub>3</sub>)Pz]Cu}<sub>3</sub>, {[3-(CF<sub>3</sub>),5-(Me)Pz]Cu}<sub>3</sub>, {[3-(CF<sub>3</sub>),5-(Ph)Pz]Cu}<sub>3</sub>, {[3,5-(CF<sub>3</sub>)<sub>2</sub>Pz]Cu}<sub>3</sub>, and {[3,5-(*i*-Pr)<sub>2</sub>Pz]Cu}<sub>3</sub>

	{[3-(CF <sub>3</sub> )Pz]Cu} <sub>3</sub>	{[3-(CF <sub>3</sub> ),5-(Me)Pz]Cu} <sub>3</sub>	{[3-(CF <sub>3</sub> ),5-(Ph)Pz]Cu} <sub>3</sub>	{[3,5-(CF <sub>3</sub> ) <sub>2</sub> Pz]Cu} <sub>3</sub>	{[3,5-( <i>i</i> -Pr) <sub>2</sub> Pz]Cu} <sub>3</sub>
empirical formula	C <sub>12</sub> H <sub>6</sub> Cu <sub>3</sub> F <sub>9</sub> N <sub>6</sub>	C <sub>15</sub> H <sub>12</sub> Cu <sub>3</sub> F <sub>9</sub> N <sub>6</sub>	C <sub>30</sub> H <sub>18</sub> Cu <sub>3</sub> F <sub>9</sub> N <sub>6</sub>	C <sub>15</sub> H <sub>3</sub> Cu <sub>3</sub> F <sub>18</sub> N <sub>6</sub>	C <sub>27</sub> H <sub>45</sub> Cu <sub>3</sub> N <sub>6</sub>
formula weight	595.85	637.93	824.12	799.85	644.31
temperature	100(2) K	100(2) K	100(2) K	100(2) K	100(2) K
wavelength	0.71073 Å	0.71073 Å	0.71073 Å	0.71073 Å	0.71073 Å
crystal system	monoclinic	monoclinic	monoclinic	triclinic	monoclinic
space group	<i>P</i> 2 <sub>1</sub> / <i>c</i>	<i>Cc</i>	<i>P</i> 2 <sub>1</sub> / <i>c</i>	<i>P</i> 1	<i>P</i> 2 <sub>1</sub> / <i>c</i>
unit cell dimensions					
<i>a</i>	15.0852(7) Å	12.7722(5) Å	11.7498(4) Å	9.1553(4) Å	14.3989(14) Å
<i>b</i>	18.0948(9) Å	22.3549(9) Å	19.5123(7) Å	11.3906(5) Å	13.4806(13) Å
<i>c</i>	13.1160(6) Å	7.4500(3) Å	13.1595(5) Å	12.2324(5) Å	17.2240(16) Å
$\alpha$	90°	90°	90°	66.4070(10)°	90°
$\beta$	100.7710(10)°	107.7660(10)°	90.6880(10)°	74.4530(10)°	112.324(2)°
$\gamma$	90°	90°	90°	78.5470(10)°	90°
volume	3517.1(3) Å <sup>3</sup>	2025.69(14) Å <sup>3</sup>	3016.80(19) Å <sup>3</sup>	1120.21(8) Å <sup>3</sup>	3092.7(5) Å <sup>3</sup>
<i>Z</i>	8	4	4	2	4
density (calcd)	2.251 Mg/m <sup>3</sup>	2.092 Mg/m <sup>3</sup>	1.814 Mg/m <sup>3</sup>	2.371 Mg/m <sup>3</sup>	1.384 Mg/m <sup>3</sup>
absorption coefficient	3.699 mm <sup>-1</sup>	3.219 mm <sup>-1</sup>	2.185 mm <sup>-1</sup>	2.992 mm <sup>-1</sup>	2.069 mm <sup>-1</sup>
<i>F</i> (000)	2304	1248	1632	768	1344
<i>R</i> 1, <i>wR</i> 2 [ <i>I</i> > 2 $\sigma$ ( <i>I</i> )]	0.0598, 0.1467	0.0220, 0.0583	0.0310, 0.0789	0.0356, 0.0939	0.0248, 0.0657
<i>R</i> 1, <i>wR</i> 2 (all data)	0.0949, 0.1699	0.0226, 0.0585	0.0348, 0.0809	0.0383, 0.0968	0.0279, 0.0672

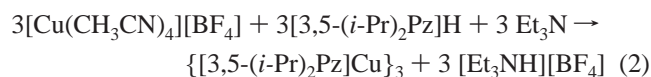
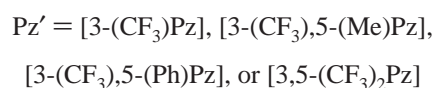
double-beam UV–vis–NIR spectrophotometer for solutions of crystalline samples prepared in HPLC-grade acetonitrile using standard 1 cm quartz cuvettes. Luminescence and lifetime studies for frozen solutions were conducted for selected samples by placing a 5 mm Suprasil quartz cylindrical tube containing the appropriate solution in a liquid nitrogen-filled dewar flask with a Suprasil quartz cold finger and then inserting this setup in the sample compartment of the PTI instrument.

## Results and Discussion

**Synthesis of Copper(I) Pyrazolates.** The reaction of copper(I) oxide and fluorinated pyrazoles, [3-(CF<sub>3</sub>)Pz]H, [3-(CF<sub>3</sub>),5-(Me)Pz]H, and [3-(CF<sub>3</sub>),5-(Ph)Pz]H, in benzene containing a few drops of acetonitrile leads to the corresponding copper(I) pyrazolates, {[3-(CF<sub>3</sub>)Pz]Cu}<sub>3</sub>, {[3-(CF<sub>3</sub>),5-(Me)Pz]Cu}<sub>3</sub>, and {[3-(CF<sub>3</sub>),5-(Ph)Pz]Cu}<sub>3</sub>, respectively, in high yield (eq 1). We have reported the synthesis of {[3,5-(CF<sub>3</sub>)<sub>2</sub>Pz]Cu}<sub>3</sub> following a similar method using just benzene as the solvent.<sup>5</sup> However, the addition of a few drops of acetonitrile improves the reproducibility and leads to consistently high yields. The {[3,5-(*i*-Pr)<sub>2</sub>Pz]Cu}<sub>3</sub> was obtained in 88% yield by a reaction between [Cu(CH<sub>3</sub>CN)<sub>4</sub>][BF<sub>4</sub>] and {[3,5-(*i*-Pr)<sub>2</sub>Pz]H in the presence of NEt<sub>3</sub> (eq 2). While this work was underway, the synthesis of {[3,5-(*i*-Pr)<sub>2</sub>Pz]Cu}<sub>3</sub> via a different route (i.e., using [3,5-(*i*-Pr)<sub>2</sub>Pz]Na and CuCl; yield = 37%) was reported by Fujisawa et al.<sup>12</sup> The {[3,5-(Me)<sub>2</sub>Pz]Cu}<sub>3</sub> was prepared by the published method,<sup>3</sup> but the purification was achieved by a more convenient and efficient vacuum sublimation process, rather than by manually separating the crystals from the crude mixture as described previously.



where



{[3-(CF<sub>3</sub>)Pz]Cu}<sub>3</sub>, {[3-(CF<sub>3</sub>),5-(Me)Pz]Cu}<sub>3</sub>, {[3-(CF<sub>3</sub>),5-(Ph)Pz]Cu}<sub>3</sub>, {[3,5-(CF<sub>3</sub>)<sub>2</sub>Pz]Cu}<sub>3</sub>, and {[3,5-(*i*-Pr)<sub>2</sub>Pz]Cu}<sub>3</sub> are soluble in most common organic solvents, such as benzene, toluene, THF, hexane, and CH<sub>2</sub>Cl<sub>2</sub>. Compound {[3,5-(Me)<sub>2</sub>Pz]Cu}<sub>3</sub>, as indicated above, is insoluble in organic solvents. It is an air-stable solid. The relative air stability of the other copper adducts also merits comment. On the basis of our observations, {[3-(CF<sub>3</sub>),5-(Me)Pz]Cu}<sub>3</sub> and {[3-(CF<sub>3</sub>),5-(Ph)Pz]Cu}<sub>3</sub> are quite air stable in the solid state as well as in solution. They survive in solution without decomposition for several weeks. {[3-(CF<sub>3</sub>),5-(Me)Pz]Cu}<sub>3</sub> is the more stable compound of the two. Trimeric {[3-(CF<sub>3</sub>)Pz]Cu}<sub>3</sub> is the least air-stable solid of all the fluorinated copper(I) complexes described in this work. It decomposes easily in solution as well as in the solid state. Even though nonfluorinated, {[3,5-(*i*-Pr)<sub>2</sub>Pz]Cu}<sub>3</sub> is relatively air stable in the solid state (for 2–3 days); once dissolved in organic solvents, it quickly decomposes, forming a green solution.

The <sup>19</sup>F NMR spectra of {[3-(CF<sub>3</sub>)Pz]Cu}<sub>3</sub> and {[3-(CF<sub>3</sub>),5-(Ph)Pz]Cu}<sub>3</sub> show only one signal each, with a chemical shift that is very close to that of the respective free ligand. Similarly, apart from the disappearance of the peak corresponding to the pyrazole N–H, other proton resonances in the <sup>1</sup>H NMR spectra do not show a notable shift going from the free pyrazoles to the respective copper adducts, {[3-(CF<sub>3</sub>)Pz]Cu}<sub>3</sub> and {[3-(CF<sub>3</sub>),5-(Ph)Pz]Cu}<sub>3</sub>. Interestingly, {[3-(CF<sub>3</sub>),5-(Me)Pz]Cu}<sub>3</sub> displays two broad peaks in the <sup>19</sup>F NMR spectrum. The methyl groups also appear as two signals close to one another in the <sup>1</sup>H NMR spectrum.

**X-ray Crystal Structures.** Single-crystal X-ray analysis of {[3-(CF<sub>3</sub>)Pz]Cu}<sub>3</sub> reveals a trinuclear structure (Figure 1) that features an asymmetrically oriented pyrazolyl group; the substituents at the pyrazolyl group's 3- and 5-positions (H and CF<sub>3</sub>) do not show a regular, alternating pattern. The pyrazolyl-bridged copper ions feature a linear geometry. The nine-membered Cu<sub>3</sub>N<sub>6</sub> metallacycle is essentially planar. There are long inter-triangle contacts involving the copper atoms forming extended chains (Figure 1). These Cu...Cu distances range from 3.100 to 3.482 Å. The intratrimer Cu...Cu separations within the copper triangles (“[Cu<sub>3</sub>]” units) range from 3.214 to 3.264 Å. These distances are much longer than the estimated sum of the

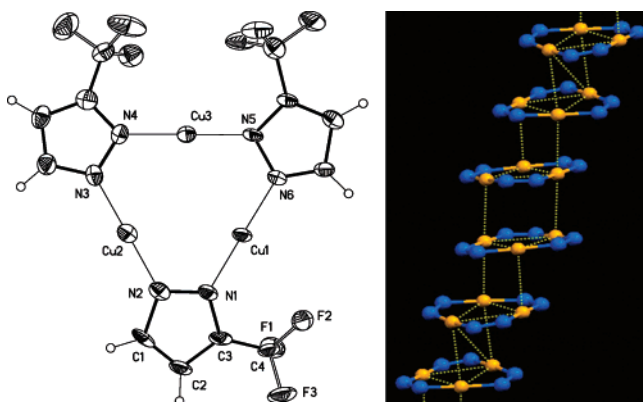


**Figure 1.** X-ray crystal structure of {[3-(CF<sub>3</sub>)Pz]Cu}<sub>3</sub> showing the labeling scheme of a molecular unit (left) and the packing of the Cu<sub>3</sub>N<sub>6</sub> metallacycles (right).

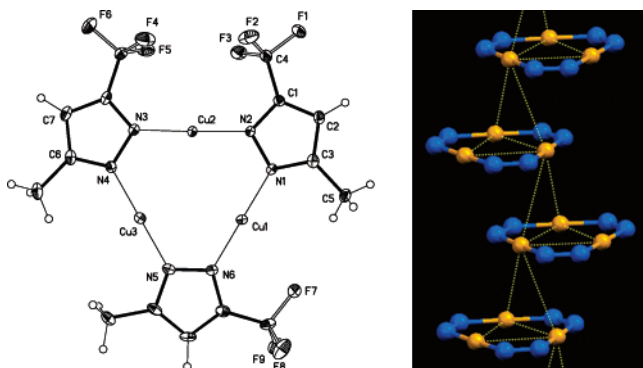


**Figure 2.** X-ray crystal structure of {[3-(CF<sub>3</sub>),5-(Me)Pz]Cu}<sub>3</sub> showing the labeling scheme of a molecular unit (left) and the packing of the Cu<sub>3</sub>N<sub>6</sub> metallacycles (right).

van der Waals radii of two copper atoms (2.80 Å) or the Cu–Cu distance in the open-shell metallic copper (2.556 Å).<sup>35</sup>

The X-ray crystal structure of {[3-(CF<sub>3</sub>),5-(Me)Pz]Cu}<sub>3</sub> is illustrated in Figure 2. This molecule also exhibits asymmetrically oriented CF<sub>3</sub> groups and does not show alternating (CF<sub>3</sub>, Me, CF<sub>3</sub>, Me, ...) pattern in the periphery. The copper ions feature a linear geometry. The nine-membered Cu<sub>3</sub>N<sub>6</sub> metallacycle is essentially planar. The [Cu<sub>3</sub>] units form extended chains (Figure 2). The intertrimer Cu⋯Cu separations range from 3.704 to 3.915 Å. The Cu⋯Cu separations within the [Cu<sub>3</sub>] units range from 3.201 to 3.245 Å.

The solid-state structure of {[3-(CF<sub>3</sub>),5-(Ph)Pz]Cu}<sub>3</sub> (Figure 3) reveals a typical triangular arrangement of copper atoms with pyrazolyl moieties occupying the edge positions. Just as in {[3-(CF<sub>3</sub>)Pz]Cu}<sub>3</sub> and {[3-(CF<sub>3</sub>),5-(Me)Pz]Cu}<sub>3</sub>, the arrangement of the pyrazolyl groups in {[3-(CF<sub>3</sub>),5-(Ph)Pz]Cu}<sub>3</sub> is not symmetrical. The copper atoms are linearly coordinated by the two nitrogens of the [3-(CF<sub>3</sub>),5-(Ph)Pz]<sup>−</sup> ligands. The nine-membered Cu<sub>3</sub>N<sub>6</sub> metallacycle shows significant deviation from planarity, perhaps as a result of the adverse steric effects of having the CF<sub>3</sub> and Ph substituents on the neighboring pyrazolyl ligands. The {[3,5-(Ph)<sub>2</sub>Pz]Cu}<sub>3</sub> compound also exhibits a distorted Cu<sub>3</sub>N<sub>6</sub> metallacycle. The intratrimer Cu⋯Cu separations within the [Cu<sub>3</sub>] units of {[3-(CF<sub>3</sub>),5-(Ph)Pz]Cu}<sub>3</sub> range from 3.147 to 3.258 Å. The inter-triangle contacts between copper atoms are rather long (3.848 and 4.636 Å, alternating with one another in the infinite zigzag chains of trimers; see

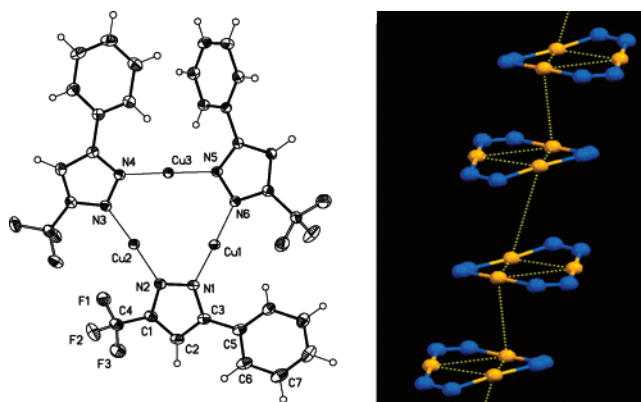


**Figure 3.** X-ray crystal structure of {[3-(CF<sub>3</sub>),5-(Ph)Pz]Cu}<sub>3</sub> showing the labeling scheme of a molecular unit (left) and the packing of the Cu<sub>3</sub>N<sub>6</sub> metallacycles (right).

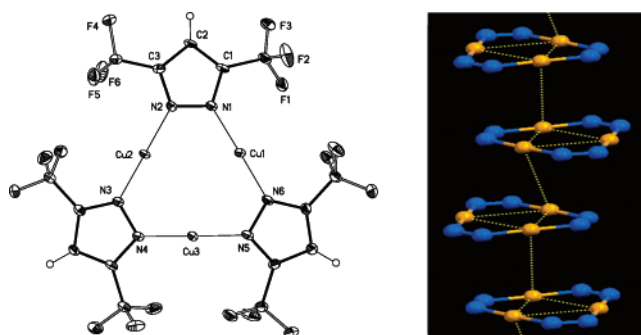


**Figure 4.** X-ray crystal structure of {[3,5-(CF<sub>3</sub>)<sub>2</sub>Pz]Cu}<sub>3</sub> showing the labeling scheme of a molecular unit (left) and the packing of the Cu<sub>3</sub>N<sub>6</sub> metallacycles (right).

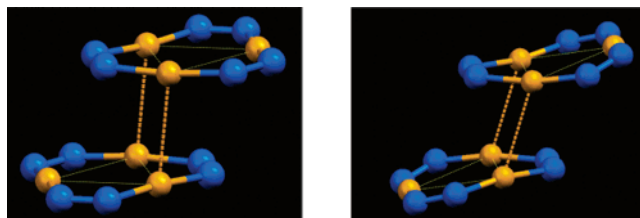


**Figure 5.** Packing of the Cu<sub>3</sub>N<sub>6</sub> metallacycles in {[3,5-(Me)<sub>2</sub>Pz]Cu}<sub>3</sub> (left) and {[3,5-(*i*-Pr)<sub>2</sub>Pz]Cu}<sub>3</sub> (right).

Figure 3). The extended packing of the [Cu<sub>3</sub>] units of {[3-(CF<sub>3</sub>),5-(Ph)Pz]Cu}<sub>3</sub> is similar to that observed in {[3,5-(CF<sub>3</sub>)<sub>2</sub>Pz]Cu}<sub>3</sub>. However, {[3,5-(CF<sub>3</sub>)<sub>2</sub>Pz]Cu}<sub>3</sub> features a planar nine-membered metallacycle (Figure 4) and somewhat shorter intertrimer Cu⋯Cu separations (3.813 and 3.987 Å, based on the data collected at 100 K).

The X-ray crystal structure of the nonfluorinated adduct, {[3,5-(Me)<sub>2</sub>Pz]Cu}<sub>3</sub>, was reported earlier.<sup>3</sup> To make sure that we use well-defined material with known solid-state structures for the luminescence work, we re-collected the data for the {[3,5-(Me)<sub>2</sub>Pz]Cu}<sub>3</sub> crystals obtained by the new sublimation method. The solid-state structure of the isopropyl analogue, {[3,5-(*i*-Pr)<sub>2</sub>Pz]Cu}<sub>3</sub>, was also determined at 100 K. The unit cell parameters are similar to those observed at room temperature for {[3,5-(Me)<sub>2</sub>Pz]Cu}<sub>3</sub> and at 208 K for {[3,5-(*i*-Pr)<sub>2</sub>Pz]Cu}<sub>3</sub>.<sup>3,12</sup> Both of these copper adducts show significant Cu⋯Cu interactions between the [Cu<sub>3</sub>] units, leading to the formation of isolated dimers of trimers (Figure 5). The shortest intertrimer Cu⋯Cu distances in {[3,5-(Me)<sub>2</sub>Pz]Cu}<sub>3</sub> and {[3,5-(*i*-Pr)<sub>2</sub>Pz]Cu}<sub>3</sub> are 2.946 and 2.989 Å, respectively. The intertrimer Cu⋯Cu

(35) (a) Bondi, A. J. *Phys. Chem.* **1964**, *68*, 441–451. (b) Winter, M. <http://www.webelements.com/>, 2004.

**Table 2.** Bond Distances (Å) and Bond Angles (deg) for Selected Pyrazolotocopper(I) Trimers

	{[3-(CF <sub>3</sub> )Pz]Cu} <sub>3</sub>	{[3-(CF <sub>3</sub> ),5-(Me)Pz]Cu} <sub>3</sub>	{[3-(CF <sub>3</sub> ),5-(Ph)Pz]Cu} <sub>3</sub>	{[3,5-(CF <sub>3</sub> ) <sub>2</sub> Pz]Cu} <sub>3</sub>	{[3,5-(Me) <sub>2</sub> Pz]Cu} <sub>3</sub>
Cu–N	1.845(8)–1.876(7)	1.852(3)–1.863(3)	1.8604(19)–1.8653(18)	1.855(2)–1.863(2)	1.845(4)–1.858(4)
Cu···Cu (intra)	3.214–3.264	3.201–3.245	3.147–3.258	3.218–3.247	3.195–3.257
Cu···Cu (inter)	3.100–3.482	3.704–3.915	3.848–4.636	3.813–3.987	2.946
N–Cu–N	174.5(3)–178.2(3)	178.07(12)–178.97(12)	174.17(8)–175.83(8)	178.39(10)–178.58(10)	173.4(2)–175.3(2)
ref	this work	this work	this work	this work	ref 3
	{[3,4,5-(Me) <sub>3</sub> Pz]Cu} <sub>3</sub>	{[3,5-( <i>i</i> -Pr) <sub>2</sub> Pz]Cu} <sub>3</sub>	{[3,5-(Ph) <sub>2</sub> Pz]Cu} <sub>3</sub>	{[2-(3-Pz)Py]Cu} <sub>3</sub>	
Cu–N	1.848(4)–1.855(4)	1.8448(10)–1.8628(10)	2.041(7)–2.105(7)	1.864(7)–1.895(7)	
Cu···Cu (intra)	3.212	3.195–3.235	3.280–3.406	3.52	
Cu···Cu (inter)	3.069	2.989	5.400	2.905	
N–Cu–N	173.9(2)–174.6(2)	169.84(4)–176.89(5)	169.2(3)–178.6(3)	166.5(3)–170.8(3)	
ref	ref 10	this work	ref 7	ref 16	

contacts of {[3,5-(Me)<sub>2</sub>Pz]Cu}<sub>3</sub> are nearly orthogonal to the [Cu<sub>3</sub>] planes. In contrast, the two [Cu<sub>3</sub>] units of {[3,5-(*i*-Pr)<sub>2</sub>Pz]Cu}<sub>3</sub> adopt a more flattened chair (i.e., a “lazy boy” recliner) arrangement with intratrimer Cu···Cu separations ranging from 3.195 to 3.235 Å.

Overall, {[3-(CF<sub>3</sub>)Pz]Cu}<sub>3</sub>, {[3-(CF<sub>3</sub>),5-(Me)Pz]Cu}<sub>3</sub>, and {[3-(CF<sub>3</sub>),5-(Ph)Pz]Cu}<sub>3</sub> represent rare copper(I) pyrazolates featuring fluorinated substituents. Only a few other trimetallic copper(I) pyrazolates have been reported. These include [3,5-(Me)<sub>2</sub>,4-(X)Pz]Cu<sub>3</sub> (where X = H, Cl, Br, I, Me),<sup>3,4,10</sup> {[2-(3-Pz)Py]Cu}<sub>3</sub>,<sup>16</sup> [3,5-(Ph)<sub>2</sub>Pz]Cu<sub>3</sub>,<sup>7</sup> [3,5-(*p*-Me-Ph)<sub>2</sub>Pz]Cu<sub>3</sub>,<sup>1</sup> [3,5-(*p*-Cl-Ph)<sub>2</sub>Pz]Cu<sub>3</sub>,<sup>1</sup> {[3,5-(Me)<sub>2</sub>,4-(NO<sub>2</sub>)Pz]Cu}<sub>3</sub>,<sup>8</sup> {[3,5-(*i*-Pr)<sub>2</sub>Pz]Cu}<sub>3</sub>,<sup>12</sup> and the highly fluorinated complex, {[3,5-(CF<sub>3</sub>)<sub>2</sub>Pz]Cu}<sub>3</sub>.<sup>5</sup> The number of such complexes that have been characterized using X-ray crystallography is even fewer among the aforementioned compounds.

Selected bond distances and angles of trimeric copper(I) pyrazolates are listed in Table 2. In general, despite the weakly donating nature of fluorinated pyrazoles, there is essentially no difference between the Cu–N bond distances of the fluorinated versus nonfluorinated systems. In the absence of adverse steric interactions, the inter-triangle Cu···Cu contacts appear to be shorter in the nonfluorinated systems. For example, {[3,5-(*i*-Pr)<sub>2</sub>Pz]Cu}<sub>3</sub> and {[3,5-(Me)<sub>2</sub>Pz]Cu}<sub>3</sub> show Cu···Cu separations between [Cu<sub>3</sub>] units at 2.9–3.0 Å. {[3,4,5-(Me)<sub>3</sub>Pz]Cu}<sub>3</sub> also has short Cu···Cu separations (see Table 2). The intertrimer Cu···Cu contacts in these compounds result in the formation of dimers of [Cu<sub>3</sub>] units. The 3,5-diphenyl-substituted analogue, {[3,5-(Ph)<sub>2</sub>Pz]Cu}<sub>3</sub>, represents an exception.<sup>7</sup> It features severely distorted, fairly well-separated [Cu<sub>3</sub>] units, perhaps as a result of the adverse steric effects of having two bulky Ph substituents on neighboring pyrazolyl ligands.

The fluorinated systems form chains of [Cu<sub>3</sub>] units with closest intertrimer Cu···Cu contacts ranging from 3.100 Å (as in {[3-(CF<sub>3</sub>)Pz]Cu}<sub>3</sub>) to 3.848 Å (for {[3-(CF<sub>3</sub>),5-(Ph)Pz]Cu}<sub>3</sub>). The nonfluorinated system, {[3,5-(Me)<sub>2</sub>,4-(NO<sub>2</sub>)Pz]Cu}<sub>3</sub>, also packs as chains of [Cu<sub>3</sub>] with intertrimer Cu···Cu separations of 3.261 Å. Although this compound does not have fluorinated substituents such as CF<sub>3</sub>, on the pyrazole rings, it has nitro groups that are even more electron-withdrawing. We note that {[3,5-(*i*-Pr)<sub>2</sub>Pz]Cu}<sub>3</sub> and {[3,5-(CF<sub>3</sub>)<sub>2</sub>Pz]Cu}<sub>3</sub> contain pyrazolyl ligands bearing substituents that are somewhat similar sterically<sup>36,37</sup> but rather different electronically.<sup>33</sup> Therefore, the structures of these two compounds may provide some clues as to how ligand electronic effects influence the packing of [Cu<sub>3</sub>] units. As mentioned above, the nonfluorinated {[3,5-(*i*-Pr)<sub>2</sub>Pz]Cu}<sub>3</sub> exhibits shorter Cu···Cu contacts and dimers of [Cu<sub>3</sub>] units,

whereas the fluorinated analogue features significantly longer Cu···Cu separations and chains of [Cu<sub>3</sub>] units. The pyrazoles in the two compounds, {[3,4,5-(Me)<sub>3</sub>Pz]Cu}<sub>3</sub> and {[3,5-(Me)<sub>2</sub>,4-(NO<sub>2</sub>)Pz]Cu}<sub>3</sub>, are also close sterically but somewhat different electronically. They show a similar trend; that is, {[3,4,5-(Me)<sub>3</sub>Pz]Cu}<sub>3</sub> forms dimers of [Cu<sub>3</sub>] units, while {[3,5-(Me)<sub>2</sub>,4-(NO<sub>2</sub>)Pz]Cu}<sub>3</sub> forms chains of [Cu<sub>3</sub>] with longer Cu···Cu distance. These data seem to indicate that electron-withdrawing groups weaken the intertrimer Cu···Cu contacts and favor long-range interactions in infinite chains of trimers instead of dimers of trimers.

The intratrimer and intertrimer Cu<sup>I</sup>···Cu<sup>I</sup> separations observed for the trinuclear species herein are to be placed in the proper perspective as to what extent do they constitute bonding interactions. This is important because the topic of Cu–Cu bonding in Cu(I) complexes has elicited a great deal of discussion and controversy.<sup>38</sup> Work by Cotton and co-workers has established the absence of a Cu<sup>I</sup>–Cu<sup>I</sup> bond<sup>39</sup> in the covalent sense known for complexes in which the transition metal has partially occupied d-orbitals, for which M–M bonds with a bond order of up to four are known.<sup>40</sup> This absence of “significant covalent bonding” has been concluded to be the case even when Cu<sup>I</sup>···Cu<sup>I</sup> separations are extremely short—as short as 2.35 Å!<sup>39</sup> A combination of strong Cu<sup>I</sup>–ligand bonding and very small bite distances (e.g., 2.2 Å) of the bridging ligands leads to the short Cu<sup>I</sup>···Cu<sup>I</sup> contacts in such cases. Plentiful examples exist for short Cu<sup>I</sup>···Cu<sup>I</sup> separations that are largely dictated either by ligand assistance or electrostatic interactions (see refs 39 and 41 and relevant citations therein). Nevertheless, there are some studies that suggest genuine intramolecular cuprophilicity based on spectroscopic evidence that includes resonance Raman bands attributed to  $\nu_{\text{Cu–Cu}}$ .<sup>42</sup> Thus, we conclude that bridging ligands and electrostatic interactions may obscure any genuine cuprophilicity in such situations. The intratrimer Cu<sup>I</sup>···Cu<sup>I</sup> contacts in the trinuclear {[3-(R),5-(R')Pz]Cu}<sub>3</sub> complexes herein fall into this category because the bridging pyrazolate ligands may provide significant assistance that could obscure any significant Cu<sup>I</sup>···Cu<sup>I</sup> interactions. On the other hand, there are cases where relatively short Cu<sup>I</sup>···Cu<sup>I</sup> separations are

(36) Smart, B. E. *ACS Monograph* **1995**, 187, 979–1010.(37) O'Hagan, D.; Rzepa, H. S. *Chem. Commun.* **1997**, 645–652.(38) Carvajal, M. A.; Alvarez, S.; Novoa, J. J. *Chem.—Eur. J.* **2004**, 10, 2117–2132.(39) (a) Cotton, F. A.; Feng, X.; Matusz, M.; Poli, R. *J. Am. Chem. Soc.* **1988**, 110, 7077–7083. (b) Cotton, F. A.; Feng, X.; Timmons, D. *J. Inorg. Chem.* **1998**, 37, 4066–4069. (c) Clerac, R.; Cotton, F. A.; Daniels, L. M.; Gu, J.; Murillo, C. A.; Zhou, H. C. *Inorg. Chem.* **2000**, 39, 4488–4493.(40) Cotton, F. A.; Walton, R. A. *Multiple Bonds Between Metal Atoms*, 2nd ed.; Oxford University Press: Oxford, U.K., 1992.(41) Poblet, J.-M.; Benard, M. *Chem. Commun.* **1998**, 11, 1179–1180.(42) See, for example: (a) Che, C. M.; Mao, Z.; Miskowski, V. M.; Tse, M. C.; Chan, C. K.; Cheung, K. K.; Phillips, D. L.; Leung, K. H. *Angew. Chem., Int. Ed.* **2000**, 39, 4084–4088. (b) Fu, W. F.; Gan, X.; Che, C. M.; Cao, Q. Y.; Zhou, Z. Y.; Zhu, N. N. *Y. Chem.—Eur. J.* **2004**, 10, 2228–2236.



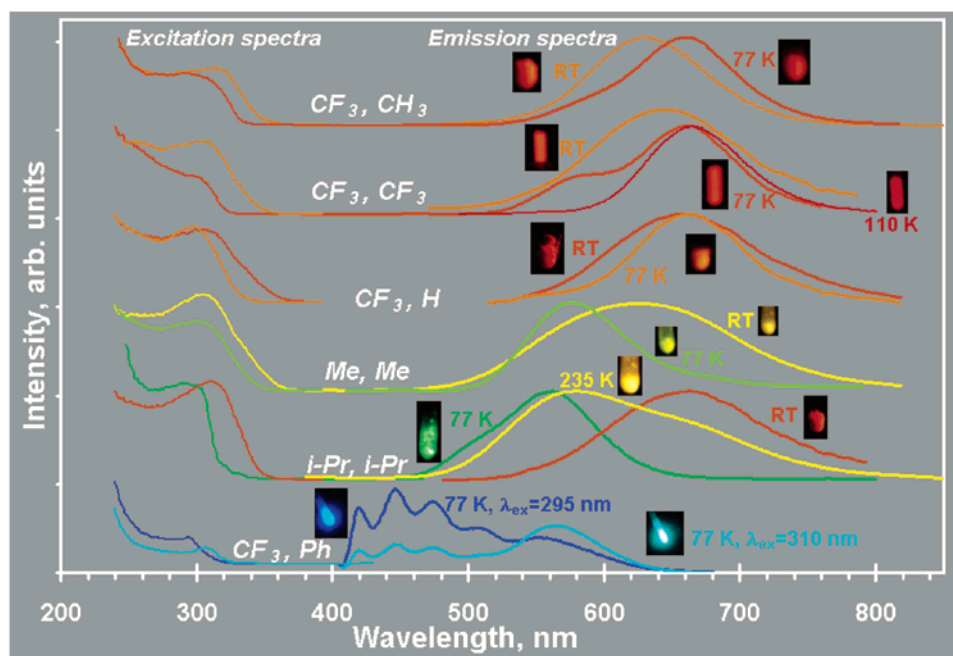


**Figure 6.** Luminescence spectra for single crystals of trinuclear  $\{[3-(R),5-(R')Pz]Cu\}_3$  complexes. The compounds are identified by the R and R' substituents. The spectra were acquired using the optical cryostat setup and are normalized and offset for clarity purposes. Photographs are shown for crystals packed in Suprasil quartz tubes while being exposed to UV light with the appropriate wavelength at room temperature (RT), immediately after removal from a liquid nitrogen bath (77 K) and at an intermediate temperature where relevant while the sample is warming but before reaching RT.

due to a genuine cuprophilicity that is unassisted by bridging ligands or electrostatics; the shortest such separations are in the range of 2.9–3.0 Å.<sup>16,17,43</sup> This cuprophilic bonding, however, is not covalent bonding with a bond order of one; otherwise, these distances would be much shorter since the covalent radius of Cu(I) has been estimated to be only ca. 1.13 Å,<sup>44</sup> plus there would be some chemical sense from an electronic structure standpoint to justify the formation of a covalent single bond between two  $d^{10}$  atoms. Instead, this bonding falls into the general category of *metallophilic bonding*, which has been reviewed by Pyykkö<sup>45</sup> and is most well-known for Au(I) compounds, largely owing to the work of Schmidbaur, who first coined the term “aurophilic attraction” to describe this type of bonding.<sup>46</sup> Metallophilic bonding has been attributed to correlation effects that are strengthened by relativistic effects.<sup>45</sup> Rigorous theoretical treatments reported to date estimate that pure cuprophilic bonding is in the range of ca. 3.5–4 kcal/mol for the dimeric models studied.<sup>47,48</sup> The intertrimer  $Cu^I \cdots Cu^I$  interactions in the trinuclear  $\{[3-(R),5-(R')Pz]Cu\}_3$  complexes herein fall into this category of genuine unassisted cuprophilic bonding. One way this bonding manifests itself is through the unassisted dimerization of  $[Cu_3]$  units in crystals of the nonfluorinated complexes,  $\{[3,5-(i-Pr)_2Pz]Cu\}_3$  and  $\{[3,5-(Me)_2Pz]Cu\}_3$ . In addition to the aforementioned short intertrimer  $Cu^I \cdots Cu^I$  distances, further insights can be gained from

the geometry in these dimers of trimers. A close inspection of Figure 5 (as well as appropriate manipulations of the crystallographic cif files) reveals that the two Cu atoms involved in intertrimer cuprophilic interactions in each trimer are “attracted” to the other two Cu atoms in the adjacent trimer, leading to deviation from planarity of the two  $Cu_3N_6$  metallacycles. A similar situation has been encountered for  $\{[2-(3-Pz)Py]Cu\}_3$ , which also exhibits a dimer of trimer structure with a chair conformation.<sup>16</sup> Further crystallographic arguments that demonstrate genuine cuprophilicity in such dimer of trimer structures are found in ref 16, which we support. In a theoretical study, Poblet and Benard argued for the significance and genuine nature of cuprophilic interactions in such dimer of trimer structures relative to other cases in which cuprophilicity was claimed; they estimated conservatively a total stabilization of ca. 6 kcal/mol owing to cuprophilicity in each dimer of trimers.<sup>41,49</sup> The theoretical arguments in refs 41 and 47 suggest that unassisted cuprophilic bonding should be accounted for even at rather long distances, such as 4.5 Å. This brings us to the second way by which genuine unassisted cuprophilic bonding manifests itself, that is, through the formation of infinite linear chains of  $[Cu_3]$  units in crystals of the fluorinated complexes herein. Despite the rather long crystallographic intertrimer  $Cu^I \cdots Cu^I$  distances, the long-range and cooperative nature of such interactions in the crystalline solid state lends significant overall stabilization given the aforementioned theoretical arguments, even if such interactions may be rather weak on a per-unit basis. As the following section illustrates, the significance of even the weakest cases of genuine cuprophilic interactions is multiplied in the low-lying electronic excited states that give rise to fascinating luminescence behavior.

(43) Kohn, R. D.; Seifert, G.; Pan, Z.; Mahon, M. F.; Kociok-Kohn, G. *Angew. Chem., Int. Ed.* **2003**, *42*, 793–796.

(44) Bayler, A.; Schier, A.; Bowmaker, G. A.; Schmidbaur, H. *J. Am. Chem. Soc.* **1996**, *118*, 7006–7007.

(45) Pyykkö, P. *Chem. Rev.* **1997**, *97*, 599–636.

(46) (a) Schmidbaur, H. *Gold Bull.* **1990**, *23*, 11–21. (b) Schmidbaur, H. *Chem. Soc. Rev.* **1995**, 391–400. (c) Grohmann, A.; Schmidbaur, H. In *Comprehensive Organometallic Chemistry II*; Abel, E. W., Stone, F. G. A., Wilkinson, G., Eds.; Pergamon: Oxford, 1995; Vol. 3, Chapter 1. (d) Schmidbaur, H. *Gold: Progress in Chemistry, Biochemistry and Technology*; Wiley: New York, 1999.

(47) Pyykkö, P.; Runeberg, N.; Mendizabal, F. *Chem.—Eur. J.* **1997**, *3*, 1451–1465.

(48) Hermann, H. L.; Boche, G.; Schwerdtfeger, P. *Chem.—Eur. J.* **2001**, *7*, 5333–5342.

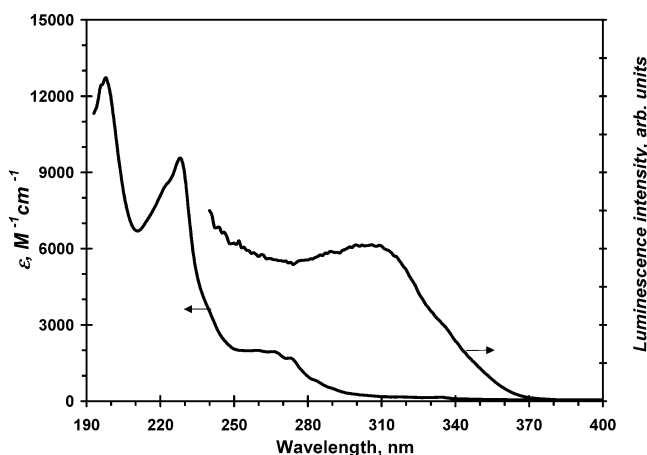
(49) We deem the estimation in ref 41 to be “conservative” because: (a) it only considers intertrimer unassisted cuprophilic interactions, (b) it considers only 50% of the MP2 stabilization, and (c) it assumes no cooperativity, despite evidence to the contrary in several other studies of metallophilic bonding.



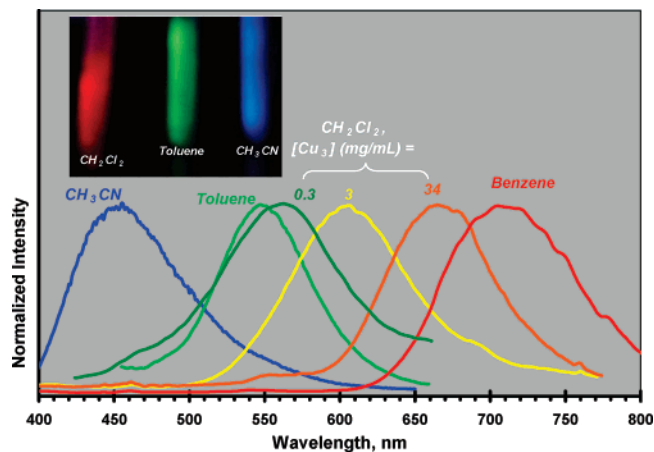
**Table 3.** Summary of the Photophysical Parameters for Crystals of Pyrazolotocopper(I) Trimers Studied

compound	temp	$\lambda_{\text{em}}^{\text{max}}$ (nm)	$\lambda_{\text{exc}}$ (nm) <sup>a</sup>	$\tau$ ( $\mu\text{s}$ )	SS ( $\text{cm}^{-1}$ ) <sup>b</sup>	fwhm ( $\text{cm}^{-1}$ ) <sup>c</sup>
{[3-(CF <sub>3</sub> ),5-(Me)Pz]Cu} <sub>3</sub>	RT	634	315	49.5 ± 1.0	16000	2260
	77 K	659	308	62.2 ± 1.9	17300	1940
{[3,5-(CF <sub>3</sub> ) <sub>2</sub> Pz]Cu} <sub>3</sub>	RT	645	306	52.6 ± 0.8	17200	2880
	77 K	663	302	64.4 ± 1.0	18000	1760
{[3-(CF <sub>3</sub> )Pz]Cu} <sub>3</sub>	RT	659	306	51.0 ± 3.8	17500	2690
	77 K	663	297	53.2 ± 3.2	18600	2000
{[3,5-(Me) <sub>2</sub> Pz]Cu} <sub>3</sub>	RT	656	304	50.1 ± 2.9	17700	4220 <sup>d</sup>
	77 K	577	299	68.5 ± 1.5	16100	2440
{[3,5-( <i>i</i> -Pr) <sub>2</sub> Pz]Cu} <sub>3</sub>	RT	662	309	28.0 ± 1.1	17300	2850
	77 K	562	292	57.8 ± 0.7	16500	2250
{[3-(CF <sub>3</sub> ),5-(Ph)Pz]Cu} <sub>3</sub>	77 K <sup>e</sup>	565	306	107 ± 4	15000	2120
	77 K <sup>f</sup>	447	294	5080 ± 88	11600	

<sup>a</sup> Major lowest-energy feature. <sup>b</sup> Apparent Stokes' shift.<sup>50</sup> <sup>c</sup> Full-width at half-maximum for unstructured emissions. <sup>d</sup> Total broadening for two strongly overlapping bands fit to two Gaussians with fwhm of 3310 and 2810  $\text{cm}^{-1}$ ; see text. <sup>e</sup> Unstructured emission. <sup>f</sup> Structured emission.

**Figure 7.** A comparison between the luminescence excitation spectrum for crystals with the absorption spectrum for solutions of {[3-(CF<sub>3</sub>)Pz]Cu}<sub>3</sub>.

**Photophysical Properties.** Figure 6 shows the solid-state luminescence spectra for single crystals of the compounds in this study. All of these copper(I) pyrazolates exhibit bright luminescence upon exposure to UV radiation. The observed lifetimes in the microsecond regime (Table 3) suggest phosphorescence. The consistent increase in the lifetime values upon cooling from room temperature to 77 K suggests a reduction in the nonradiative decay rate, as expected. The luminescence bands are hugely red-shifted from the corresponding lowest-energy excitations, rather broad, and unstructured (with one exception noted below) even at low temperatures for single crystals (conditions that favor resolution). These observations are consistent with an assignment to a metal-centered phosphorescence for the unstructured emissions. The excitation peaks shown likely represent spin-forbidden transitions because they are significantly red-shifted from the major absorption bands seen in solution, as illustrated in the representative example shown in Figure 7 for the {[3-(CF<sub>3</sub>)Pz]Cu}<sub>3</sub> compound. Hence, the large energy separation between the lowest-energy luminescence excitation feature and the unstructured emission band for each compound seems to represent a bona fide Stokes' shift.<sup>50</sup> The fact that rather broad (fwhm = ca.  $2\text{--}3 \times 10^3 \text{ cm}^{-1}$ ) unstructured emission bands that are separated by  $15.0\text{--}18.6 \times 10^3 \text{ cm}^{-1}$  from the corresponding lowest-energy excitation bands are observed for crystals of the trinuclear complexes herein (Table 3) suggests that the phosphorescent excited states

**Figure 8.** Representative emission spectra for frozen solutions (77 K) of {[3,5-(CF<sub>3</sub>)<sub>2</sub>Pz]Cu}<sub>3</sub> versus solvent and concentration. Lifetimes at  $\lambda_{\text{max}}$  (right-to-left, respectively) are  $80 \pm 3$ ,  $62 \pm 1$ ,  $52 \pm 2$ ,  $98 \pm 2$ ,  $84 \pm 1$ , and  $21 \pm 1 \mu\text{s}$ . The photograph shows selected CH<sub>2</sub>Cl<sub>2</sub>, toluene, and CH<sub>3</sub>CN frozen solutions in Suprasil quartz tubes exposed to UV light immediately after removal from a liquid nitrogen bath. The temperature increase on removing the sample from the bath changes the emission color of the 34 mg/mL CH<sub>2</sub>Cl<sub>2</sub> solution from orange to red. Luminescence colors of frozen solutions in other solvents that are not shown include red (cyclohexane or pentane), orange (methanol or ethanol), and blue (acetone).

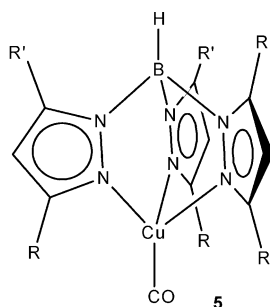
involved are distorted rather hugely! A logical explanation for such a huge distortion is a dramatic compression of Cu<sup>••</sup>Cu separations in the phosphorescent state from the rather long separations (vide supra) in the ground state because the lowest-energy excited states in aggregates of d<sup>10</sup> complexes involve transitions from  $\sigma_{\text{nd}}^*$  antibonding filled orbitals to vacant bonding molecular orbitals arising from the  $(n + 1)s/p$  subshells. The presence of Cu<sup>••</sup>Cu interactions should decrease the triplet energy of Cu(I) from the 22 649  $\text{cm}^{-1}$  value for the free ion,<sup>51</sup> especially in the phosphorescent excited state. Hence, the unstructured emissions may be assigned to intratrimer or intertrimer Cu<sup>••</sup>Cu interactions because the compounds herein exhibit both (Table 2). An intertrimer distortion is expected to be more facile than an intratrimer distortion because the former involves lattice vibrations (phonons), which are much lower in energy than molecular vibrations. Representative frozen solutions data are illustrated in Figure 8, showing unstructured emissions whose energies (and colors) are solvent-dependent and which exhibit red shifts upon increasing the concentration in some solvents to approach the solid-state behavior. These results are consistent with relating the unstructured emissions to intertrimer interactions. Hence, we assign the emitting states responsible for the unstructured emissions to be triplet Cu–Cu bonded  $^*[\text{Cu}_3]_2$  excimers. Enhanced M–M bonding in the excited state has been reported for Cu(I) and other d<sup>10</sup> luminescent materials,<sup>52</sup> leading to the formation of excimers

(50) Nevertheless, we will refer to the Stokes' shifts in this paper as "apparent" ones (Table 3) because it is hard to establish the exact states involved in the absorption and emission processes. An ongoing theoretical study addresses the exact states involved in the absorption and emission transitions.

(51) Weighted average for the three  $^3D_{3,2,1}$  spin-orbit states. See: Moore, C. E. *Atomic Energy Levels*. Nat. Bur. Stand: Washington, 1958; Circ. 467, Vol. III.

(52) See, for example: (a) Hollingsworth, G.; Barrie, J. D.; Dunn, B.; Zink, J. I. *J. Am. Chem. Soc.* **1988**, *110*, 6569–6570. (b) Vitale, M.; Ryu, C. K.; Palke, W. E.; Ford, P. C. *Inorg. Chem.* **1994**, *33*, 561–566. (c) Rawashdeh-Omary, M. A.; Omary, M. A.; Patterson, H. H.; Fackler, J. P., Jr. *J. Am. Chem. Soc.* **2001**, *123*, 11237–11247. (d) Omary, M. A.; Patterson, H. H. *J. Am. Chem. Soc.* **1998**, *120*, 7696–7705. (e) Omary, M. A.; Hall, D. R.; Shankle, G. E.; Siemiarczuk, A.; Patterson, H. H. *J. Phys. Chem. B* **1999**, *103*, 3845–3853.

Chart 2



$$R = CF_3, R' = CF_3; \nu_{CO} = 2137 \text{ cm}^{-1}$$

$$R = CF_3, R' = H; \nu_{CO} = 2100 \text{ cm}^{-1}$$

$$R = Me, R' = Me; \nu_{CO} = 2066 \text{ cm}^{-1}$$

$$R = i\text{-Pr}, R' = i\text{-Pr}; \nu_{CO} = 2056 \text{ cm}^{-1}$$

and exciplexes that are analogous to those in organic compounds.<sup>53</sup> M–M-bonded excimers and exciplexes are now becoming commonly recognized for closed-shell transition-metal species.<sup>52,54</sup> The assignment of the unstructured luminescence bands of the trimeric complexes herein to intertrimer Cu···Cu interactions explains the lack of an intuitive trend upon varying the substituents. If the luminescence bands were due to transitions within an individual molecular unit of the trimeric complex, one would expect a much more pronounced substituent effects due to the expected influence on the electronic structure of fluorinated versus nonfluorinated R groups. The pyrazolyl ring substituents can alter the electron density on copper, as evident from the  $\nu_{CO}$  data for the related tris(pyrazolyl)-boratocopper(I) carbonyl complexes (see **5** for several examples).<sup>33</sup> The central role of intertrimer interactions on the luminescence bands is consistent with the assignments given by Raptis et al.<sup>55</sup> and Fackler et al.<sup>56</sup> for trinuclear Au(I) pyrazolate and carbeniate complexes, respectively. Another striking feature in the solid-state luminescence data in Figure 6 is “luminescence thermochromism”, the extent of which varies among the different compounds. The most dramatic changes are for  $\{[3,5\text{-}(i\text{-Pr})_2\text{Pz}]\text{Cu}\}_3$ , in which cooling from room temperature to 77 K changes the emission color from orange ( $\lambda_{\text{max}} = 662 \text{ nm}$ ) to green ( $\lambda_{\text{max}} = 562 \text{ nm}$ ), while at intermediate temperatures, the sample’s emission appears yellow. This compound was, hence, selected for a detailed temperature-dependent luminescence study, the results of which are illustrated in Figure 9. These data show that there are actually three emission bands for  $\{[3,5\text{-}(i\text{-Pr})_2\text{Pz}]\text{Cu}\}_3$  with maxima near 510 (green), 560 (lime green), and 660 nm (orange). The relative intensities of these bands change with temperature. The green

band can be resolved from the more dominant lime green band at temperatures below  $\sim 100 \text{ K}$ . The relative intensity of the green band decreases gradually upon heating between 4 and 100 K, and the band disappears at higher temperatures. The lime green emission becomes essentially the only major emission between 100 and 230 K, but a further temperature increase results in a gradual generation of the orange emission. The combination of the lime green and orange emission bands between 230 and 250 K gives the yellow emission color, while further heating toward room temperature results in the dominance of the orange emission. The lifetime data indicate that all of the three aforementioned bands are due to phosphorescence with lifetime values that increase for each band upon cooling; this increase is especially substantial in the coldest temperature range,  $4 < T (\text{K}) < 30$ , at which a very sharp slope is seen due to the annihilation of the nonradiative decay rate at such temperatures. Extrapolation of this slope to 0 K results in an estimated value for the radiative decay constant ( $k_{\text{rad}}$ ) of  $\sim 3.3 \times 10^3 \text{ s}^{-1}$  for the green band at  $\sim 510 \text{ nm}$  and  $1.7 \times 10^3 \text{ s}^{-1}$  for the lime green band at  $\sim 560 \text{ nm}$ . The differences in  $k_{\text{rad}}$ ,  $\tau$  values at different temperatures, and luminescence excitation profiles suggest that these two bands are poorly coupled with one another, a situation similar to that encountered by the studies of Ford et al. for the two emission bands responsible for the luminescence thermochromism of  $\text{Cu}_4\text{L}_4\text{X}_4$  (L = aromatic amine; X = halide) clusters.<sup>30,52b</sup> In contrast, the 660 nm orange band seems to be coupled with the 560 nm lime green band since the two bands have essentially indistinguishable excitation profiles and lifetime values (Figure 9), so these two bands are likely in a thermal equilibrium. Analysis of the changes in the relative intensities of these two bands in the 225–270 K temperature range (relative peak areas from a two Gaussian fit at each temperature) gives an activation energy of  $4850 \text{ cm}^{-1}$  (13.9 kcal/mol) for the internal conversion from the triplet state responsible for the lime green emission to the triplet state responsible for the orange emission. Other samples besides  $\{[3,5\text{-}(i\text{-Pr})_2\text{Pz}]\text{Cu}\}_3$  also show luminescence thermochromism, principally due to changes in the relative intensities of two emission bands. Note in Figure 6 that  $\{[3\text{-}(\text{CF}_3)_2,5\text{-}(\text{Me})\text{Pz}]\text{Cu}\}_3$ ,  $\{[3,5\text{-}(\text{CF}_3)_2\text{Pz}]\text{Cu}\}_3$  and  $\{[3\text{-}(\text{CF}_3)\text{Pz}]\text{Cu}\}_3$  exhibit shoulders in the yellow region that become more well-defined at 77 K in addition to the dominant peak in the red region. For  $\{[3,5\text{-}(\text{CF}_3)_2\text{Pz}]\text{Cu}\}_3$ , the orange emission color at 77 K is due to the combination of these two peaks, but heating toward room temperature leads to the disappearance of the yellow shoulder, leaving only the red emission at intermediate temperatures in the range of  $\sim 100\text{--}240 \text{ K}$ ; band broadening at higher temperatures, including room temperature, leads to an orange emission color. Similarly, the emission color changes for  $\{[3,5\text{-}(\text{CH}_3)_2\text{Pz}]\text{Cu}\}_3$  between lime green to yellow are due to a change in the relative intensity of two peaks with the higher-energy peak becoming more dominant upon cooling. The very broad emission of  $\{[3,5\text{-}(\text{CH}_3)_2\text{Pz}]\text{Cu}\}_3$  at room temperature (fwhm =  $4220 \text{ cm}^{-1}$ ) gave an excellent fit ( $R^2 = 0.9985$ ;  $\chi^2 = 1.942 \times 10^{-4}$ ) to two Gaussian peaks with maxima at  $17\,049$  ( $\sim 587 \text{ nm}$ ) and  $15\,320 \text{ cm}^{-1}$  ( $\sim 653 \text{ nm}$ ) and fwhm values of  $3310$  and  $2810 \text{ cm}^{-1}$ , respectively.

The above results indicate that the luminescence thermochromism in  $\{[3\text{-}(R),5\text{-}(R')\text{Pz}]\text{Cu}\}_3$  complexes occurs as a result of changes in the relative intensities between multiple emission bands. Hence, we assign these changes to be a result of thermal

- (53) (a) *The Exciplex*; Gordon, M., Ware, W. R., Eds; Academic Press: New York, 1975. (b) Turro, N. J. *Modern Molecular Photochemistry*; Benjamin/Cummings: Menlo Park, CA, 1978; pp 135–146. (c) Lamola, A. A. In *Energy Transfer and Organic Photochemistry*; Lamola, A. A., Turro, N. J., Eds.; Wiley-Interscience: New York, 1969; pp 54–60. (d) Lowry, T. H.; Schuller-Richardson, K. *Mechanism and Theory in Organic Chemistry*; Harper & Row: New York, 1981; pp 919–925. (e) Kopecky, J. *Organic Photochemistry: A Visual Approach*; VCH: New York, 1991; pp 38–40. (f) Michl, J.; Bonacic-Koutecky, V. *Electronic Aspects of Organic Photochemistry*; Wiley: New York, 1990; pp 274–286.
- (54) For reviews about M–M-bonded excimers and exciplexes, see: (a) Nagle, J. K. *Spectrum* **1999**, 12, 15. (b) Horváth, A.; Stevenson, K. L. *Coord. Chem. Rev.* **1996**, 153, 57–82. (c) Omary, M. A.; Patterson, H. H. *Electronic Spectroscopy: Luminescence Theory. Encyclopedia of Spectroscopy & Spectrometry*; Academic Press: London, U.K., 2000; pp 1186–1207. (d) Callear, A. B. *Chem. Rev.* **1987**, 87, 335–355.
- (55) Yang, G.; Raptis, R. G. *Inorg. Chem.* **2003**, 42, 261–263.
- (56) Rawashdeh-Omary, M. A.; Omary, M. A.; Fackler, J. P., Jr.; Galassi, R.; Pietroni, B. R.; Burini, A. *J. Am. Chem. Soc.* **2001**, 123, 9689–9691.

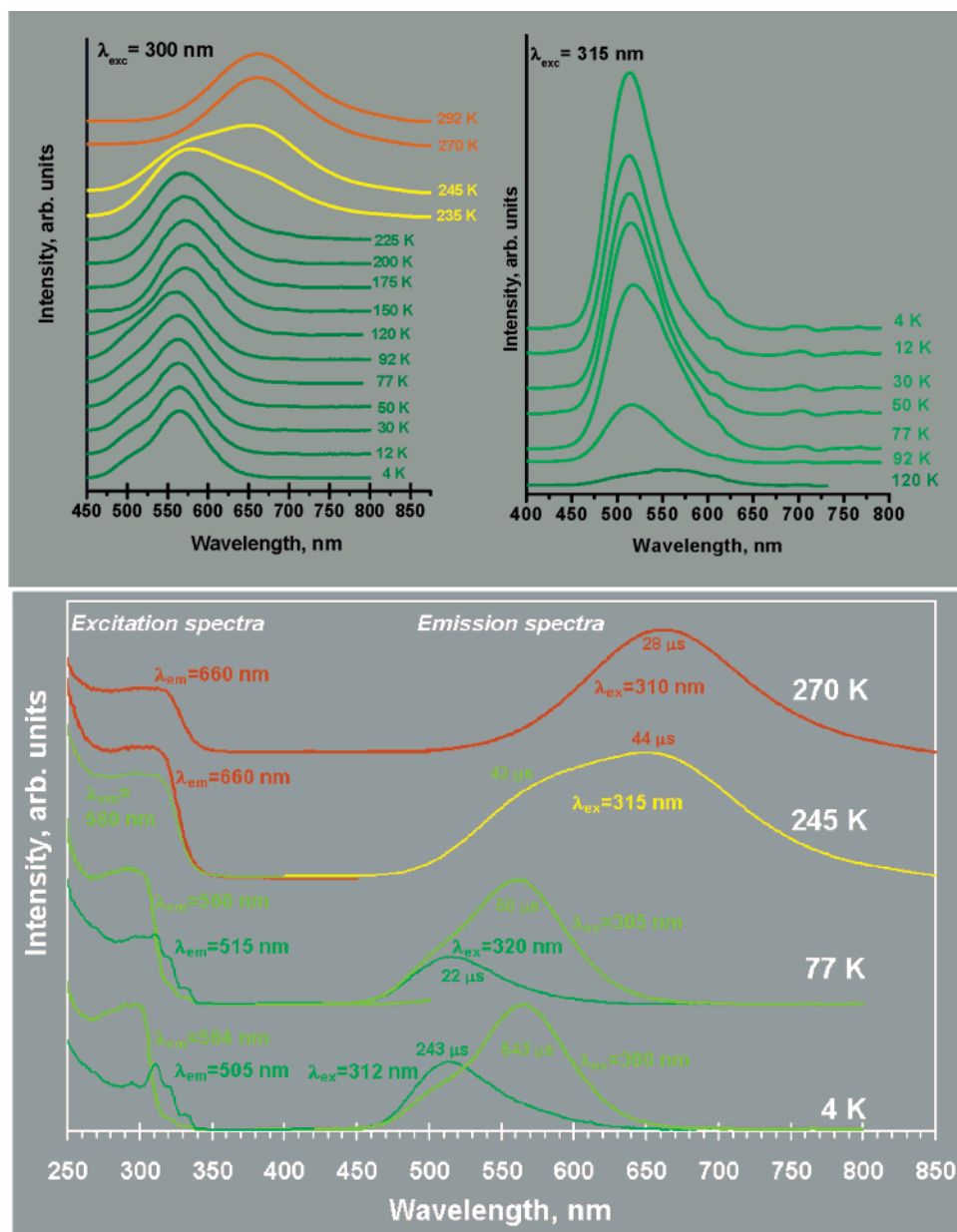


**Figure 9.** Temperature-dependent luminescence data for crystals of  $\{[3,5-(i\text{-Pr})_2\text{Pz}]\text{Cu}\}_3$ . The spectra were acquired using the optical cryostat setup and are normalized and offset for clarity purposes. The relative intensities are accurate for the traces at the same temperature. All lifetime data were generated with 285 nm laser excitation and have errors similar to those in Table 3 (1–8%).

relaxation between different emitting states, as opposed to being due to factors such as thermal compression of  $\text{M}\cdots\text{M}$  distances, which are known for other closed-shell coordination compounds that show  $\text{M}\cdots\text{M}$  packing in the solid state.<sup>57</sup> Although similar compressions (i.e., leading to the formation of more closely linked dimers of trimers) do occur in the compounds herein upon cooling (e.g., the shortest intertrimer  $\text{Cu}\cdots\text{Cu}$  distances for  $\{[3,5-(\text{CF}_3)_2\text{Pz}]\text{Cu}\}_3$  and  $\{[3,5-(\text{Me})_2\text{Pz}]\text{Cu}\}_3$  at RT and 100 K are 3.879 and 3.813 Å, and 2.946 Å and 2.874 Å, respectively), the direct impact of such slight compressions is usually<sup>57</sup> a gradual red shift in the emission maximum of one

band upon cooling, while the above data clearly show that this is not the cause of the major luminescence thermochromism changes observed. There is a consistent trend in the above data to suggest that the higher-energy emitting states at lower temperatures are depopulated upon heating, while the lower-energy emitting states responsible for the lower-energy emissions at higher temperatures are populated. Figure 10 illustrates the photophysical model that we propose for the trinuclear compounds herein according to the above data and discussion. The occurrence of multiple emitting states is not a very common phenomenon in luminescent molecular compounds owing to the so-called Kasha's rule,<sup>58</sup> but it is certainly not unprecedented. One relevant example of a precedent is represented by  $\text{Cu}_4\text{L}_4\text{X}_4$  clusters, whose luminescence thermochromism was attributed by Ford et al. to changes in the relative intensities between two

(57) See, for example: (a) Gliemann, G.; Yersin, H. *Struct. Bonding* **1985**, 62, 87–153. (b) Connick, W. B.; Henling, L. M.; Marsh, R. E.; Gray, H. B. *Inorg. Chem.* **1996**, 35, 6261–6265. (c) Nagasundaram, N.; Roper, G.; Biscoe, J.; Chai, J. W.; Patterson, H. H.; Blom, N.; Ludi, A. *Inorg. Chem.* **1986**, 25, 2947–2951. (d) Burini, A.; Bravi, R.; Fackler, J. P., Jr.; Galassi, R.; Grant, T. A.; Omary, M. A.; Pietroni, B. R.; Staples, R. J. *Inorg. Chem.* **2000**, 39, 3158–3165.

(58) Kasha, M. *Discuss. Faraday Soc.* **1950**, 9, 14–19.



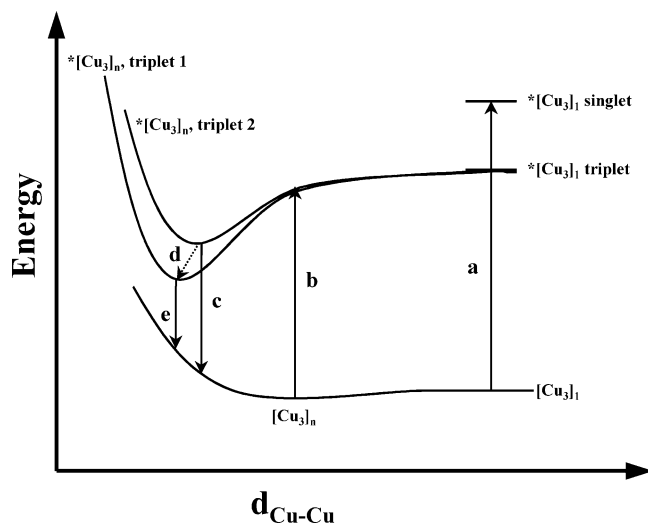


**Figure 10.** Proposed photophysical model for the trinuclear Cu(I) pyrazolates. The transitions shown depict: (a) solution absorption bands (e.g., Figure 7, left); (b) solid-state excitation bands (e.g., Figure 7, right); (c) higher-energy emission bands (e.g., the green emission of  $\{[3,5-(i\text{-Pr})_2\text{Pz}]_3\text{Cu}\}_3$  in Figure 6); (d) internal conversion to a lower triplet; and (e) lower-energy emission bands (e.g., the orange emission of  $\{[3,5-(i\text{-Pr})_2\text{Pz}]_3\text{Cu}\}_3$  in Figure 6).

emitting states of different origins, a cluster-centered lower-energy band and an interligand charge-transfer higher-energy band.<sup>30,52b</sup> Another example is represented by molecular emissions in the mercury vapor, for which multiple emission bands have been attributed to various bound states of the  $^*\text{Hg}_2$  excimer and various bound states of the  $^*\text{Hg}_3$  trimer exciplex.<sup>54d,59</sup> The model in Figure 10 is suggested for  $\{[3-(\text{R}),5-(\text{R}')\text{Pz}]_3\text{Cu}\}_3$  complexes that exhibit two unstructured emissions, but the same principle is valid for  $\{[3,5-(i\text{-Pr})_2\text{Pz}]_3\text{Cu}\}_3$  with slight modifications. Because the compound exhibits three unstructured emissions, a third bound state is suggested for  $\{[3,5-(i\text{-Pr})_2\text{Pz}]_3\text{Cu}\}_3$ . Also, the multiple excitation and emission maxima do not necessarily correlate with one another energy wise for this compound. Figure 9 shows that the higher-energy green emission peaks at 4 and 77 K are associated with lower-energy excitation peaks compared to those for the lime green luminescence peaks. This anomaly has been noticed earlier in species that exhibit similar multiple luminescence bands due to excited-state M–M bonding, such as  $^*[\text{Ag}(\text{CN})_2^-]_n$ <sup>52d</sup> and  $^*\text{Hg}_n$ <sup>54d,59</sup> excimers and exciplexes, and also for  $\text{Cu}_4\text{L}_4\text{X}_4$  clusters.<sup>30,52b</sup>

The remarkable luminescence behavior of the trinuclear complexes herein and the sensitivity of the emission to various factors warrant further comments. The data are reminiscent of several novel optical phenomena that have been reported individually for other metal complexes. These phenomena are observed *collectively*, together with yet another new phenomenon even *in a single compound*, as we illustrate for a compound that we have studied in some detail,  $\{[3,5-(\text{CF}_3)_2\text{Pz}]_3\text{Cu}\}_3$ . The “luminescence thermochromism” phenomenon is seen rather dramatically for various solids (Figures 6 and 9), including  $\{[3,5-(\text{CF}_3)_2\text{Pz}]_3\text{Cu}\}_3$ . Solutions of  $\{[3,5-(\text{CF}_3)_2\text{Pz}]_3\text{Cu}\}_3$  show bright phosphorescence when cooled to liquid nitrogen temperature. When they are removed from the liquid nitrogen bath, the emission color often changes as the sample starts to warm, but then the emission intensity decreases dramatically and essentially

disappears when the solution warms to room temperature. There is a consistent shift to a lower emission energy that we have seen on heating frozen solutions to higher temperatures to approach the fluid state (see Figure 8 caption for an illustration). This illustrates another case of “luminescence rigidochromism”, which was first noted by Wrighton and Morse for  $\text{ClRe}(\text{CO})_3$ - (diimine) complexes<sup>60</sup> and is now known for several classes of coordination compounds.<sup>30,61,62</sup> The solvent dependence of the emission color of glassy solutions (Figure 8) illustrates a dramatic case of “luminescence solvatochromism”, which is related to a few fascinating observations for several classes of  $d^{10}$  and  $d^8$  complexes that have been reported to interact with solvent molecules to change their emission colors.<sup>63</sup> What is unusual about the results here is not only the selectivity even for similar solvents (e.g., toluene vs benzene) and the versatility of solvents in which  $\{[3,5-(\text{CF}_3)_2\text{Pz}]_3\text{Cu}\}_3$  shows luminescence solvatochromism but also the qualitative changes in the visible emission colors and spectra when the concentration is varied in the same solvent. The most striking changes were seen in dichloromethane, in which the luminescence was tuned to essentially all visible colors between blue and red by varying the concentration. This “concentration luminochromism” in which *multiple visible colors* are emitted by controlling the luminophore concentration is an unprecedented optical phenomenon, to our knowledge. The closest analogy is to the changes from monomer to excimer emission in polynuclear aromatic organic molecules<sup>53</sup> and to the changes from smaller to larger  $^*[\text{Ag}(\text{CN})_2^-]_n$  or  $^*[\text{Au}(\text{CN})_2^-]_n$  oligomers<sup>52c–e</sup> upon increasing the concentration, but these cases were not as dramatic in covering multiple emissions in the visible region for the same compound as the case shown in Figure 8. The emission color changes with solvent, temperature, concentration, and/or excitation wavelength were not limited to  $\{[3,5-(\text{CF}_3)_2\text{Pz}]_3\text{Cu}\}_3$ . Figure 11 illustrates some of these changes for other compounds. We attribute the changes in the luminescence energies with concentration to  $^*[\text{Cu}_3]_n$  excimers and exciplexes that vary in  $n$  and/or the number of intertrimer  $\text{Cu}\cdots\text{Cu}$  interactions between adjacent trimers. A red shift in the emission energy upon increasing the concentration would take place, for example, due to the formation of a  $^*[\text{Cu}_3]_3$  trimer exciplex instead of a  $^*[\text{Cu}_3]_2$  excimer, or due to the formation of a  $^*[\text{Cu}_3]_2$  excimer with two intertrimer  $\text{Cu}-\text{Cu}$  bonds instead of a  $^*[\text{Cu}_3]_2$

- (60) Wrighton, M.; Morse, D. L. *J. Am. Chem. Soc.* **1974**, *96*, 998–1003.  
 (61) For more examples, see: (a) Vogler, A.; Kunkely, H. *J. Am. Chem. Soc.* **1986**, *108*, 7211–7212. (b) McKiernan, J.; Pouxviel, J. C.; Dunn, B.; Zink, J. I. *J. Phys. Chem.* **1989**, *93*, 2129–2133. (c) Franville, A.-C.; Dunn, B.; Zink, J. I. *J. Phys. Chem. B* **2001**, *105*, 10335–10339. (d) Watts, R. J.; Missimer, D. *J. Am. Chem. Soc.* **1978**, *100*, 5350–5357. (e) Zuleta, J. A.; Bevilacqua, J. M.; Rehm, J. M.; Eisenberg, R. *Inorg. Chem.* **1992**, *31*, 1332–1337. (f) Colombo, M. G.; Hauser, A.; Gudel, H. U. *Top. Curr. Chem.* **1994**, *171*, 143–171. (g) Rawlins, K. A.; Lees, A. J.; Fuerniss, S. J.; Papatomas, K. I. *Chem. Mater.* **1996**, *8*, 1540–1544. (h) Clark, I. P.; George, M. W.; Johnson, F. P. A.; Turner, J. J. *Chem. Commun.* **1996**, *13*, 1587–1588. (i) Turner, J. J.; George, M. W.; Clark, I. P.; Virrels, I. G. *Laser Chem.* **1999**, *19*, 245–251. (j) Seneviratne, J.; Cox, J. A. *Talanta* **2000**, *52*, 801–806. (k) Forster, L. S.; Rund, J. V. *Inorg. Chem. Commun.* **2003**, *6*, 78–81. (l) Fernandez, S.; Fornies, J.; Gil, B.; Gomez, J.; Lalinde, E. *Dalton Trans.* **2003**, *5*, 822–830. (m) Itokazu, M. K.; Polo, A. S.; Iha, N. Y. M. *J. Photochem. Photobiol. A* **2003**, *160*, 27–32.  
 (62) For a review, see: Lees, A. J. *Comments Inorg. Chem.* **1995**, *17*, 319–346.  
 (63) (a) White-Morris, R. L.; Olmstead, M. M.; Jiang, F.; Tinti, D. S.; Balch, A. L. *J. Am. Chem. Soc.* **2002**, *124*, 2327–2336. (b) Mansour, M. A.; Connick, W. B.; Lachicotte, R. J.; Gysling, H. J.; Eisenberg, R. *J. Am. Chem. Soc.* **1998**, *120*, 1329–1330. (c) Cariati, E.; Bu, X.; Ford, P. C. *Chem. Mater.* **2000**, *12*, 3385–3391. (d) Fernandez, E. J.; Lopez-de-Luzuriaga, J. M.; Monge, M.; Olmos, M. E.; Perez, J.; Laguna, A.; Mohamed, A. A.; Fackler, J. P., Jr. *J. Am. Chem. Soc.* **2003**, *125*, 2022–2023. (e) Kunugi, Y.; Mann, K. R.; Miller, L. L.; Exstrom, C. L. *J. Am. Chem. Soc.* **1998**, *120*, 589–590.

(59) Koperski, J.; Atkinson, J. B.; Krause, L. *J. Mol. Spectrosc.* **1998**, *187*, 181–192.



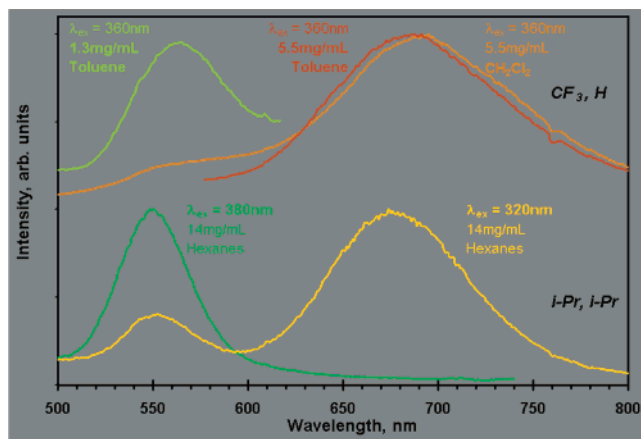


**Figure 11.** Illustration of the sensitivity of the emission spectra for frozen solutions of: (a) (top)  $\{[3-(\text{CF}_3)\text{Pz}]\text{Cu}\}_3$  to solvent and concentration, and (b) (bottom)  $\{[3,5-(i\text{-Pr})_2\text{Pz}]\text{Cu}\}_3$  to excitation wavelength. The curve colors are representative of the visible luminescence colors for the samples.

excimer with one intertrimer Cu–Cu bond. This assignment is similar to the one given by Patterson and co-workers for the excited-state oligomerization of  $\text{Ag}(\text{CN})_2^-$  and  $\text{Au}(\text{CN})_2^-$  species in solutions and doped solids.<sup>52c–e</sup> The solvatochromic changes of the luminescence spectra can thus be related to different extents of excited-state association of the  $[\text{Cu}_3]$  units, so that the emitting species in solution are  $^*[\text{Cu}_3]_n$  oligomeric excimers and exciplexes. However, one notices in Figure 8 that some frozen solution emission bands are red-shifted beyond the solid-state emission in Figure 6. Two reasons may be responsible for this result. First, it is possible that the intertrimer interactions in the glassy solutions in question lead to a lower-energy emitting state than the one in the solid state. Enhanced intermolecular interactions between  $d^{10}$  complexes in solution are not uncommon. For example, Balch and co-workers have reported that Au(I) carbene complexes that are both nonluminescent and do not exhibit intermolecular Au–Au interactions in the solid state become brightly luminescent in frozen solutions due to enhanced aggregation in solution.<sup>63a</sup> Eisenberg and co-workers have also reported the formation of luminescent species with enhanced Au–Au interactions upon sorption of solvent molecules.<sup>63b</sup> Second, formation of an exciplex between an excited-state  $^*[\text{Cu}_3]_n$  oligomer and a ground-state solvent molecule may lead to a situation in which the resulting  $^*\{[\text{Cu}_3]_n \cdot \text{solvent}\}$  exciplex is a lower-energy emitter than the  $^*[\text{Cu}_3]_n$  species alone. Che and co-workers have suggested that interactions between  $^*[\text{Au}]_2$  excimers and solvent molecules result in a red shift in the emission energies for dimeric Au(I) phosphine complexes.<sup>64</sup> The known high reactivity<sup>53,54</sup> of excimers and exciplexes coupled with the low coordination number in linear monovalent coinage metal complexes makes the formation of  $^*[\text{M}_n \cdot \text{solvent}]$  exciplexes a reasonable contention. In conclusion, the dramatic changes in the luminescence properties for frozen solutions of the trimeric Cu(I) complexes compared to those of the solid state may be attributed to both the alteration of the intertrimer interactions between adjacent  $[\text{Cu}_3]$  units as well as possible interactions with solvent molecules.

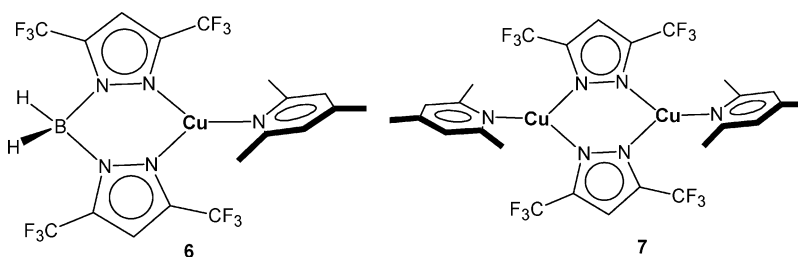
Crystals of  $\{[3-(\text{CF}_3),5-(\text{Ph})\text{Pz}]\text{Cu}\}_3$  exhibit a highly structured blue emission in addition to the lower-energy unstructured metal-centered emission. The phosphorescence lifetime is

significantly longer, by an order of magnitude, for the structured emission (Table 3). The spacing between the structured peaks is essentially uniform with an average of  $1400 \text{ cm}^{-1}$ . Several pyrazolate ring vibrations exist in that region (see the infrared data above). Hence, the structured band likely corresponds to a vibronic progression in a normal mode that is centered on the Pz ring. These results are consistent with an assignment to a Pz ligand-centered phosphorescence that is sensitized via an internal heavy atom effect for the structured emission of  $\{[3-(\text{CF}_3),5-(\text{Ph})\text{Pz}]\text{Cu}\}_3$ . We have recently communicated<sup>20</sup> that the mononuclear complexes  $[\text{H}_2\text{B}(3,5-(\text{CF}_3)_2\text{Pz})_2]\text{M}(2,4,6\text{-collidine})$  with  $\text{M} = \text{Cu}$  (**6**) and Ag exhibit such a Pz ligand-centered phosphorescence, the energy and profile of which showed indifference to the identity of the metal and agreed well with the phosphorescence bands reported<sup>65</sup> for phenyl-substituted pyrazoles. The dinuclear complex,  $\{[3,5-(\text{CF}_3)_2\text{Pz}]\text{Cu}(2,4,6\text{-collidine})\}_2$  (**7**), exhibits a very similar phosphorescence band that is slightly red-shifted from that of the mononuclear complexes,  $[\text{H}_2\text{B}(3,5-(\text{CF}_3)_2\text{Pz})_2]\text{M}(2,4,6\text{-collidine})$ .<sup>20</sup> We have suggested that the  $^3\pi-\pi^*$  emissive state is slightly perturbed by interaction with copper. A similar argument may be valid for the structured emission band of  $\{[3-(\text{CF}_3),5-(\text{Ph})\text{Pz}]\text{Cu}\}_3$  such that a triplet ligand to metal–metal charge transfer state,  $^3\text{LMMCT}$ , in the dinuclear and trinuclear complexes is possible. If the structured emission of  $\{[3-(\text{CF}_3),5-(\text{Ph})\text{Pz}]\text{Cu}\}_3$  were to be simply due to a  $^3\pi-\pi^*$  transition, one would expect a stronger overlap between the excitation and emission profiles and a smaller Stokes' shift, as is the case typically for phosphorescence in organic molecules.<sup>66</sup> Finally, it is interesting to note that the excitation profile corresponding to the green emission of  $\{[3,5-(i\text{-Pr})_2\text{Pz}]\text{Cu}\}_3$  has resolved vibronic structure at low temperatures (Figure 9). A spacing of  $\sim 1000 \text{ cm}^{-1}$  is observed, significantly lower than the  $\sim 1400 \text{ cm}^{-1}$  spacing observed in the structured emission bands of  $\{[3-(\text{CF}_3),5-(\text{Ph})\text{Pz}]\text{Cu}\}_3$ . The vibronic structure in the excitation bands must be related to an excited-state normal mode that is centered on the Pz ring instead of being due to excited-state Cu–Cu vibrations. This is because M–M vibrations, even for fully bonded excimers with excited-state M–M single bonds, usually have much lower wavenumbers of ca.  $100\text{--}150 \text{ cm}^{-1}$ .<sup>52c,54,64</sup> Thus, the lower wavenumber spacing in the excitation spectra is attributed to significant weakening of the  $\pi$  bonds within the Pz moieties upon photoexcitation. Alternatively, the progression seen in the excitation spectra of  $\{[3,5-(i\text{-Pr})_2\text{Pz}]\text{Cu}\}_3$  may be due to a different Pz ring normal mode from that seen in the emission spectra of  $\{[3-(\text{CF}_3),5-(\text{Ph})\text{Pz}]\text{Cu}\}_3$ . The IR data for the two compounds show vibrations in the regions of both progressions. Unfortunately, we have not obtained structured emission and structured excitation profiles for the same compound to make a more direct comparison. Nevertheless, the IR data do not show significant changes in the Pz vibrations between different  $\text{Cu}_3\text{Pz}'_3$  compounds that differ only in substituents. Clearly, further studies are warranted for this family of compounds in order to understand the vibrational changes associated with the electronic transitions.

(64) (a) Fu, W. F.; Chan, K. C.; Miskowski, V. M.; Che, C. M. *Angew. Chem., Int. Ed. Engl.* **1999**, *38*, 2783–2785. (b) Zhang, H. X.; Che, C. M. *Chem.—Eur. J.* **2001**, *7*, 4887–4893.

(65) (a) Swaminathan, M.; Dogra, S. K. *Spectrochim. Acta* **1983**, *39A*, 973–977. (b) Catalan, J.; Fabero, F.; Claramunt, R. M.; Santa Maria, M. D.; Foces-Foces, M. C.; Cano, F. H.; Martinez-Ripoll, M.; Elguero, J.; Sastre, R. *J. Am. Chem. Soc.* **1992**, *114*, 5039–5048.  
(66) McGlynn, S. P.; Azumi, T.; Kinoshita, M. *Molecular Spectroscopy of the Triplet State*; Prentice Hall: Englewood Cliffs, NJ, 1969.

Chart 3



### Concluding Remarks

This work describes details of efficient syntheses, structures including solid-state packing, and photophysical properties of a series of fluorinated trinuclear copper(I) pyrazolates and related nonfluorinated analogues. Reaction between copper(I) oxide and readily available fluorinated pyrazoles affords the corresponding copper(I) pyrazolates in excellent yields. X-ray data show that the fluorinated compounds,  $\{[3-(\text{CF}_3)\text{Pz}]\text{Cu}\}_3$ ,  $\{[3-(\text{CF}_3),5-(\text{Me})\text{Pz}]\text{Cu}\}_3$ ,  $\{[3-(\text{CF}_3),5-(\text{Ph})\text{Pz}]\text{Cu}\}_3$ , and  $\{[3,5-(\text{CF}_3)_2\text{Pz}]\text{Cu}\}_3$ , form trimers that pack in zigzag chains. In contrast, the nonfluorinated compounds,  $\{[3,5-(\text{Me})_2\text{Pz}]\text{Cu}\}_3$  and  $\{[3,5-(i\text{-Pr})_2\text{Pz}]\text{Cu}\}_3$ , form dimers of trimers with much shorter intertrimer  $\text{Cu}\cdots\text{Cu}$  separations than those in the fluorinated analogues. This study illustrates the significant impact of packing via  $\text{Cu}\cdots\text{Cu}$  intertrimer interactions on the photophysical properties of trinuclear Cu(I) pyrazolate complexes. Despite the inherent weakness of such closed-shell *cuprophilic* interactions in the electronic ground state, their strong enhancement in the emissive excited states is responsible for the bright luminescence bands that can be tuned across the visible region. It is amazing that fascinating luminescence properties owing to intertrimer interactions occur in compounds in which such interactions are so weak in the electronic ground state (e.g., 3.813 and 3.987 Å in  $\{[3,5-(\text{CF}_3)_2\text{Pz}]\text{Cu}\}_3$ ; 3.848 and 4.636 Å in  $\{[3-(\text{CF}_3),5-(\text{Ph})\text{Pz}]\text{Cu}\}_3$ ) such that one would be tempted to naively ignore such interactions when assigning the luminescence bands. The strong  $\text{Cu}-\text{Cu}$  bonding in many low-lying excimer-type excited states should bring down these distances to the bonding range in a manner akin to that encountered in organic excimers, for which the ground-state crystallographic requirement is that aromatic molecules must be stacked in columns or arranged in pairs with interplanar distances of  $\sim 3.5$  Å (at which obviously there is no ground-state bonding) in order to exhibit excimer-type emissions in the solid state,<sup>67</sup> and in the  $^* \text{Hg}_2$  mercury excimer for which several experimental

studies determined the ground-state distance to be 3.63–3.71 Å,<sup>54d,68</sup> which shrinks in the excited-state responsible for the well-known 335 nm excimer emission to  $2.5 \pm 0.1$  Å.<sup>68</sup>

Besides the scientific significance of the above results, the observation of bright phosphorescence at room temperature for crystals and sublimed thin films is prompting us to pursue using these types of multinuclear  $d^{10}$  pyrazolate complexes as emitting materials for MOLEDs. Indeed, preliminary experiments have led to a successful construction of a device based on  $\{[3,5-(\text{CF}_3)_2\text{Pz}]\text{Cu}\}_3$ , for which the electroluminescence spectrum showed the same orange emission band as that exhibited in the photoluminescence spectrum of the single crystals at room temperature.<sup>69</sup> Work is underway in an independent detailed electroluminescence study to optimize the device heterostructure and to test other compounds in this family as MOLED emitters. Finally, the dramatic luminescence color changes for the materials herein upon temperature and solvent variations are promising for sensor applications.

**Acknowledgment.** This work is supported by the National Science Foundation (CHE-0314666 to H.V.R.D.; CAREER Award CHE-0349313 to M.A.O.) and the Robert A. Welch Foundation (Grant Y-1289 to H.V.R.D.; Grant B-1542 to M.A.O.).

**Supporting Information Available:** X-ray crystallographic data at 100 K for  $\{[3-(\text{CF}_3)\text{Pz}]\text{Cu}\}_3$ ,  $\{[3-(\text{CF}_3),5-(\text{Me})\text{Pz}]\text{Cu}\}_3$ ,  $\{[3-(\text{CF}_3),5-(\text{Ph})\text{Pz}]\text{Cu}\}_3$ ,  $\{[3,5-(i\text{-Pr})_2\text{Pz}]\text{Cu}\}_3$ , and  $\{[3,5-(\text{CF}_3)_2\text{Pz}]\text{Cu}\}_3$  (CIF). This material is available free of charge via the Internet at <http://pubs.acs.org>.

JA0427146

- (67) For example, see: (a) Stevens, B. *Spectrochim. Acta* **1962**, *18*, 439–448. (b) Ferguson, J. *J. Chem. Phys.* **1958**, *28*, 765–768.  
 (68) (a) van Zee, R. D.; Blankespoor, S. C.; Zwier, T. S. *J. Chem. Phys.* **1988**, *88*, 4650–4654. (b) Ceccherini, S.; Moraldi, M. *Chem. Phys. Lett.* **2001**, *337*, 386–390.  
 (69) Williams, C. D.; Gnade, B. E.; Omary, M. A.; Dias, H. V. R. Unpublished results.